Food Microbiology 122 (2024) 104532

Contents lists available at ScienceDirect

Food Microbiology

journal homepage: www.elsevier.com/locate/fm

Several secondary metabolite gene clusters in the genomes of ten *Penicillium* spp. raise the risk of multiple mycotoxin occurrence in chestnuts

Marco Garello [a,b], Edoardo Piombo [c], Fabio Buonsenso [a,b], Simona Prencipe [a], Silvia Valente [a,b], Giovanna Roberta Meloni [a,b], Marina Marcet-Houben [d,e], Toni Gabaldón [d,e,f,g,**], Davide Spadaro [a,b,*]

[a] Department of Agricultural, Forest and Food Sciences (DISAFA), University of Turin, Largo Braccini 2, 10095, Grugliasco, TO, Italy
[b] AGROINNOVA – Interdepartmental Centre for the Innovation in the Agro-Environmental Sector, University of Torino, Largo Braccini 2, 10095, Grugliasco, TO, Italy
[c] Department of Forest Mycology and Plant Pathology, Swedish University of Agricultural Sciences, Almas Allé 5, 75651, Uppsala, Sweden
[d] Barcelona Supercomputing Centre (BSC-CNS), Plaça Eusebi Güell, 1-3, 08034, Barcelona, Spain
[e] Institute for Research in Biomedicine (IRB Barcelona), The Barcelona Institute of Science and Technology, Baldiri Reixac, 10, 08028 Barcelona, Spain
[f] Catalan Institution for Research and Advanced Studies (ICREA), Barcelona, Spain
[g] CIBER de Enfermedades Infecciosas, Instituto de Salud Carlos III, Madrid, Spain

ARTICLE INFO

Keywords:
Mycotoxigenic fungi
Food safety
Postharvest pathogens
phylome
LC-MS/MS
Penicillium taurinense

ABSTRACT

Penicillium spp. produce a great variety of secondary metabolites, including several mycotoxins, on food substrates. Chestnuts represent a favorable substrate for *Penicillium* spp. development. In this study, the genomes of ten *Penicillium* species, virulent on chestnuts, were sequenced and annotated: *P. bialowiezense*. *P. pancosmium*, *P. manginii*, *P. discolor*, *P. crustosum*, *P. palitans*, *P. viridicatum*, *P. glandicola*, *P. taurinense* and *P. terrarumae*. Assembly size ranges from 27.5 to 36.8 Mb and the number of encoded genes ranges from 9,867 to 12,520. The total number of predicted biosynthetic gene clusters (BGCs) in the ten species is 551. The most represented families of BGCs are non ribosomal peptide synthase (191) and polyketide synthase (175), followed by terpene synthases (87). Genome-wide collections of gene phylogenies (phylomes) were reconstructed for each of the newly sequenced *Penicillium* species allowing for the prediction of orthologous relationships among our species, as well as other 20 annotated *Penicillium* species available in the public domain. We investigated *in silico* the presence of BGCs for 10 secondary metabolites, including 5 mycotoxins, whose production was validated *in vivo* through chemical analyses. Among the clusters present in this set of species we found andrastin A and its related cluster atlantinone A, mycophenolic acid, patulin, penitrem A and the cluster responsible for the synthesis of roquefortine C/glandicoline A/glandicoline B/meleagrin. We confirmed the presence of these clusters in several of the *Penicillium* species conforming our dataset and verified their capacity to synthesize them in a chestnut-based medium with chemical analysis. Interestingly, we identified mycotoxin clusters in some species for the first time, such as the andrastin A cluster in *P. flavigenum* and *P. taurinense,* and the roquefortine C cluster in *P. nalgiovense* and *P. taurinense*. Chestnuts proved to be an optimal substrate for species of *Penicillium* with different mycotoxigenic potential, opening the door to risks related to the occurrence of multiple mycotoxins in the same food matrix.

1. Introduction

Penicillium is a genus of Ascomycetes belonging to the *Aspergillaceae* family, which, consists of 483 described species divided into 32 sections (Houbraken et al., 2020). Most *Penicillium* spp. are saprophytic, but some can act as opportunistic plant pathogens and cause postharvest diseases, such as *P. expansum* (Louw and Korsten, 2014; Yin et al., 2017), *P. crustosum* (López et al., 2016), *P. digitatum* and *P. italicum* (Arras et al., 2005). More importantly, *Penicillium* spp. can produce a great variety of secondary metabolites, which are bioactive molecules assembled from products of the primary metabolite pool (Keller, 2019). A conservative estimate indicates at least 1,300 secondary metabolites for this genus

* Corresponding author. Department of Agricultural, Forest and Food Sciences (DISAFA), University of Turin, Largo Braccini 2, 10095, Grugliasco, TO, Italy.
** Corresponding author. Barcelona Supercomputing Centre (BSC-CNS), Plaça Eusebi Güell, 1-3, 08034 Barcelona, Spain.
E-mail addresses: toni.gabaldon@bsc.es (T. Gabaldón), davide.spadaro@unito.it (D. Spadaro).

https://doi.org/10.1016/j.fm.2024.104532
Received 6 January 2024; Received in revised form 14 March 2024; Accepted 2 April 2024
Available online 4 April 2024

Table 1
Genome assembly parameters for the ten newly sequenced *Penicillium* spp. For each species it is reported the strain, isolation source, measured virulence on chestnuts, the total scaffold number, the number of scaffolds longer than 1000 bp, the size of biggest scaffold, the total genome length, the GC percentage, N50, the number of N per 100 kb, the putative coverage and the putative gene number. N50: defined as the cumulative number of longest contigs that constitutes 50 % of the assembly. Number of N per 100 kb: the number of unresolved bases per 100 kb. Source: C: chestnut; F: flour; I: indoor; PP: processing phases. Virulence: MV: moderately virulent; HV: highly virulent.

Species	*P. discolor*	*P. glandicola*	*P. crustosum*	*P. bialowiezense*	*P. pancosmium*	*P. palitans*	*P. viridicatum*	*P. manginii*	*P. terrarumae*	*P. taurinense*
Strain	3B6	3C	CAL64	CAS30	FP10	SP3	XA	YELL	MO7	CAS16
Source	I	I	F	C	C	PP	PP	C	F	PP
Virulence	HV	MV	HV	HV	MV	MV	HV	HV	HV	HV
N° scaffolds (total)	1169	232	427	113	652	1219	729	798	3645	1232
N° scaffold (>1000)	967	193	379	105	533	965	558	684	730	391
Biggest scaffold (bp)	675239	1074011	563637	1904703	717269	473831	871540	545557	905399	547406
Total length (Mb)	33.40	28.40	31.00	29.20	36.20	35.30	31.70	36.80	36.20	27.50
GC percentage	49.59	48.07	48.08	50.11	48.70	47.91	48.15	48.38	49.29	48.15
N50 (bp)	133561	379411	163626	563120	192031	105014	172019	152430	219873	169426
#N per 100 kbp	373.67	0.02	0.34	0.53	0.30	0.09	0.42	0.27	0.65	2.60
Putative coverage	394.10	566.50	485.60	439.40	361.80	373.50	444.50	346.10	267.66	379.34
Putative gene number	12325	10262	11164	11242	12657	11943	11372	12520	11893	9867

alone (Frisvad, 2015), including several mycotoxins.

Mycotoxins are fungal secondary metabolites that can pose a health hazard for humans and other vertebrates by exerting a toxic activity even at low concentrations (IC50 < 1000 μM) (Taevernier et al., 2016). These compounds can cause acute or chronic effects, whose severity depends on mycotoxin concentration, period of exposure, body mass, presence of synergistic effects and environmental factors (Freire and da Rocha, 2016). Notable examples among *Penicillium* spp. mycotoxins include ochratoxin A (Cabañes et al., 2010), patulin (Zhong et al., 2018), penitrem A (Sumarah et al., 2005), and verrucosidin (Thomas et al., 2013).

In fungi, as well as in bacteria, biosynthetic genes associated to a common secondary metabolism pathway are usually clustered in a single genetic locus (in some cases a couple of loci) called biosynthetic gene cluster (BGC) (Medema et al., 2011; Cimermancic et al., 2014). BGCs can vary considerably in size and composition, but all canonical clusters contain one or two core/backbone enzymes, which polymerize the primary metabolites into a precursor compound, and a variable number of tailoring enzymes, which further modify this compound into one or more final products. Additional genes can be present, such as genes conferring resistance, BGC-specific transcription factors and cryptic genes of unknown function (Keller, 2019). Since most secondary metabolites are only produced in response to specific combinations of factors, such as certain pH, nutritional inputs (in particular iron, carbon and nitrogen levels), light intensity and quality, temperature and oxidative stress (Macheleidt et al., 2016; Keller, 2019), which cannot be always achieved during metabolic sampling, the identification of genomically-encoded BGCs can prove useful in assessing the biosynthetic (and thus toxigenic) potential of isolates of interest.

Despite the significant economic losses caused by *Penicillium* spp. rots, as well as the health hazard posed by many of their secondary metabolites, sequence data associated with their genomes and BGC content is still incomplete. At the time of writing (December 2023) only 162 species had their genomes sequenced, of which 104 had a publicly available annotation, based on data collected from NCBI (Schoch et al., 2020) and Mycocosm (Grigoriev et al., 2014).

In this study, we aimed to provide annotated genomes for strains of ten *Penicillium* species: *P. bialowiezense*. *P. pancosmium*, *P. manginii*, *P. discolor*, *P. crustosum*, *P. palitans*, *P. viridicatum*, *P. glandicola*, *P. taurinense* and *P. terrarumae*, of which *P. glandicola*, *P. taurinense* and *P. terrarumae* have been sequenced for the first time. These species were chosen based on their virulence on chestnut among a pool of 20 *Penicillium* spp. previously isolated from fresh chestnuts, as well as chestnut derived products (Prencipe et al., 2018), which represent a favorable substrate for mycotoxigenic fungi development, especially during storage, due to their high water and starch content (Overy et al., 2003; Rodrigues et al., 2012).

In our previous paper (Prencipe et al., 2018), *Penicillium* strains were identified utilizing a multidisciplinary approach, which involved phylogenetic analysis of the ITS region, beta-tubulin, and calmodulin genes, macro-morphological analysis using three different media, and chemical evaluation to assess the *in vivo* production of 14 toxic metabolites.

Knowledge of genome composition was used to investigate *in silico* the presence of BGCs associated with selected mycotoxins, whose production was validated *in vivo* through chemical analyses.

2. Materials and methods

2.1. Fungal strains

Ten *Penicillium* spp. strains, isolated from fresh chestnuts and along the flour processing phases, pathogenic on chestnut and identified by molecular and morphological analyses (Prencipe et al., 2018; Crous et al., 2020), were selected for *de novo* genome sequencing (Table 1). Following a polyphasic approach, based on micro and macro-morphological analyses, multilocus sequence typing and secondary metabolite production, described in Prencipe et al. (2018), eight strains were identified as *P. bialowiezense* (CAS30), *P. crustosum* (CAL64), *P. discolor* (3B6), *P. glandicola* (3C), *P. manginii* (YELL), *P. palitans* (SP3), *P. pancosmium* (FP10), and *P. viridicatum* (XA). The strain CAS16 of *P. taurinense* (Crous et al., 2020), isolated from a chestnut mill, and the strain MO7 of *P. terrarumae*, isolated from chestnut flour, were identified with a similar procedure and included in this study, based on the same criteria. Fungal strains were grown on Potato Dextrose Agar plates (PDA, Merck KGaA, Darmstadt, Germany) with 50 μg/ml streptomycin (Merck KGaA) and maintained as conidial suspension at −80 °C in the Turin University Culture Collection (TUCC - http://www.tucc.unito.it/). TUCC and Bioproject NCBI identification collection numbers of isolates included in this study are reported in Suppl Table 1.

2.2. Growth of Penicillium spp. in vitro

For DNA extraction, fungal isolates were grown on Czapek Yeast

Table 2
Availability of biosynthetic gene cluster (BGCs) data for all considered mycotoxins. For each mycotoxin the presence of an identified cluster in literature is reported, as well as whether a putative orthologue of such cluster was found in any of the phylome seed species.

Metabolite	Identified BGC	Species with BGC characterized	BGC in phylome seed species
Cyclopenol	Yes[a]	- *A. nidulans* (Ishikawa et al., 2014; Kishimoto et al., 2018) - *P. thymicola* (Zou et al., 2015)	No
Cyclopenin	Yes[a]	- *A. nidulans* (Ishikawa et al., 2014; Kishimoto et al., 2018) - *P. thymicola* (Zou et al., 2015)	No
Roquefortine C	Yes	- *P. rubens* (García-Estrada et al., 2011); - *P. roqueforti* (Kosalková et al., 2015)	*P. glandicola*
Citreoviridin	Yes	- *A. nidulans* (Lin et al., 2016); - *P. citreonigrum* (Okano et al., 2020)	No
Mycophenolic acid	Yes	- *P. brevicompactum* (Regueira et al., 2011); - *P. roqueforti* (Del-Cid et al., 2016)	*P. bialowiezense*
Sulochrin	Yes[b]	- *A. terreus* (Nielsen et al., 2013) - *A. fumigatus* (Throckmorton et al., 2016)	No
Asterric acid	No	/	No
Andrastin A	Yes	- *A. oryzae* (Matsuda et al., 2013); - *P. roqueforti* (Rojas-Aedo et al., 2017)	*P. glandicola*
Meleagrin	Yes	- *P. rubens* (García-Estrada et al., 2011); - *P. roqueforti* (Kosalková et al., 2015)	*P. glandicola*
Cyclopiazonic acid	Yes	- *A. flavus* (Chang et al., 2009); - *A. parasiticus* (Chang et al., 2009); - *A. oryzae* (Kato et al., 2011)	No
Chaetoglobosin A	Yes	- *Chaetomium globosum* (Ishiuchi et al., 2013) - *P. expansum* (Zetina-Serrano et al., 2020)	*P. expansum*
Patulin	Yes	- *P. rubens* (van den Berg et al., 2008) - *A. clavatus* (Artigot et al., 2009) - *P. expansum* (Tannous et al., 2014)	*P. expansum*
Viridicatin	Yes[a]	- *A. nidulans* (Ishikawa et al., 2014; Kishimoto et al., 2018) - *P. thymicola* (Zou et al., 2015)	No
Penitrem A	Yes	- *P. simplicissimum* (Liu et al., 2015) - *P. crustosum* (Nicholson et al., 2015)	*P. flavigenum*
Palitantin	No	/	No
Ochratoxin A	Yes	- *P. nordicum* (Karolewiez and Geisen, 2004; Geisen et al., 2006) - *P. verrucosum* (Abbas et al., 2013) - *A. steynii, A. westerdijkiae, A. niger, A. carbonarius* and *A. ochraceus* (Gil-Serna et al., 2018; Wang et al., 2018)	No
Glandicoline A	Yes	- *P. rubens* (García-Estrada et al., 2011); - *P. roqueforti* (Kosalková et al., 2015)	*P. glandicola*
Glandicoline B	Yes	- *P. rubens* (García-Estrada et al., 2011); - *P. roqueforti* (Kosalková et al., 2015)	*P. glandicola*
Verrucosidin	Yes	- *P. polonicum* (Valente et al., 2021)	*P. glandicola*
Penicillic acid	No	/	No

[a] Identified as biosynthetic intermediates of the aspoquinolones biosynthetic pathway.
[b] Identified as biosynthetic intermediate of the trypacidin (in *A. fumigatus*) and geodin (in *A. terreus*) biosynthetic pathways.

Autolysate (CYA) broth (Visagie et al., 2014), without shaking, at 26 °C for 7 days, except for *P. discolor* which was grown on Potato Dextrose Broth (PDB, Merck KGaA) on a rotatory shaker (150 rpm) at the same growth conditions. The evaluation of secondary metabolites production *in vitro* was performed following previously described protocols (Visagie et al., 2014). Briefly, all the strains were inoculated on Czapek yeast autolysate (CYA) agar and yeast extract sucrose (YES) agar plates in triplicate and incubated for 7 days at 25 °C in the dark.

2.3. Genomic DNA extraction

The fungal mycelium was collected and lyophilized overnight using CoolSafe™ Pro SL11a01 (Scanvac, Allerød, Denmark)/Heto FD1.0 (De Mori Strumenti, Milan, Italy) freeze-dryer. One hundred mg of mycelium were collected in 2 mL tubes and frozen in liquid nitrogen. Two tungsten beads (diameter: 2.7 mm) were added to the mycelium that was crushed using Tissue Lyser (Qiagen, Hilden, Germany) for 1 min at 20.00 Hz speed. Then, Qiagen DNeasy Plant Mini Kit was used according to manufacturer's instruction, and the DNA was diluted in 50 μL of Tris-EDTA (TE) buffer. DNA purity was checked by spectrophotometer (Nanodrop 2000), while DNA concentration and integrity were analyzed by agarose gel electrophoresis and using Qubit™ dsDNA HS Assay Kit.

2.4. Genome sequencing

The genomes were sequenced through Illumina pair-end technology, using 2x150bp read length design and an Illumina Hiseq instrument at the genomics core facility of the Centre for Genomic Regulation (CRG) in Barcelona, Spain.

2.5. Genome assembly and annotation

Quality trimming and adapter removal of raw reads was conducted with Trimmomatic v 0.36 (Bolger et al., 2014) using default parameters. Read quality was checked with fastqc (https://www.bioinformatics.babraham.ac.uk/projects/fastqc/), and genome assembly was then performed with SPAdes v3.7.1 using the "–min-cov-cutoff auto" and "–careful" options (Bankevich et al., 2012). Abyss sealer v2.1.0 (Paulino et al., 2015) was used with default parameters to perform gap-closing, and the quality of the final assembly was verified with QUAST v 4.0 (Gurevich et al., 2013).

Gene prediction was carried out with MAKER 2.31.8 (Campbell et al., 2014), using SNAP v 2006-07-28 (http://korflab.ucdavis.edu/software.html) and Augustus v2.5.5 (Stanke et al., 2006) as *de novo* gene predictors. mRNA and protein sequences available on Genbank for the

Table 3
Number of BGCs for each of the newly annotated *Penicillium* spp. as predicted by Antismash 5.2.0, divided by core enzyme and sorted by total cluster number. NRPS: non ribosomial peptide synthase; PKS: polyketide synthase; DMATS: dimethylallyltryptophan synthase; RiPP: Ribosomally synthesized and post-translationally modified peptide. The hybrid class includes both clusters with multiple core enzymes of different classes and clusters with a single hybrid core enzyme.

Species	NRPS	PKS	Terpene	Hybrid	DMATS	RiPP	Siderophore	Total number of BGCs
Penicillium pancosmium	17	14	4	1	1	1	0	38
Penicillium. terrarumae	15	18	6	6	1	1	0	47
Penicillium manginii	21	16	4	6	0	0	1	48
Penicillium taurinense	17	18	9	5	1	0	0	50
Penicillium glandicola	13	22	8	9	1	0	0	53
Penicillium discolor	20	16	9	10	2	0	0	57
Penicillium bialowiezense	21	22	8	7	0	0	0	58
Penicillium crustosum	20	13	10	14	2	0	0	59
Penicillium palitans	21	19	15	10	3	0	0	68
Penicillium viridicatum	26	16	14	12	4	1	0	73
Total number of BGCs	**191**	**174**	**87**	**80**	**15**	**3**	**1**	**551**

species of the Citrina subgenus were used to train predictors for the species *P. manginii* and *P. pancosmium*, while sequences from the *Penicillium* subgenus were used for the other species. SNAP was trained following the suggested procedure for MAKER (http://weatherby.genetics.utah.edu/MAKER/wiki/index.php/MAKER_Tutorial_for_GMOD_Online_Training_2014#Training_ab_initio_Gene_Predictors), while Augustus was trained through the available webservice (Hoff and Stanke, 2013). Before gene prediction, repetitive sequences were masked with RepeatModeler v2.0 (Flynn et al., 2020) following the suggested procedure for gene prediction with MAKER (http://weatherby.genetics.utah.edu/MAKER/wiki/index.php/Repeat_Library_Construction–Basic). The genomes and their annotation were submitted to ENA (European Nucleotide Archive) under the project PRJEB35841 and they received the following accession numbers: *P. bialowiezense* CAS30 (GCA_902713515), *P. crustosum* CAL64 (GCA_902712905), *P. discolor* 3B6 (GCA_902713485), *P. glandicola* 3C (GCA_902713505), *P. manginii* YELL (GCA_902713545), *P. palitans* SP3 (GCA_902713495), *P. pancosmium* FP10 (GCA_902713525), *P. viridicatum* XA (GCA_902713535), *P. taurinense* CAS16 (GCA_907164605), *P. terrarumae* MO7 (GCA_907164625).

After gene prediction, putative secondary metabolism gene clusters were predicted in each of the genomes with antiSMASH version 5.2.0 (Blin et al., 2019).

2.6. Phylome generation and cladogram construction

Phylomes, complete collections of phylogenetic trees for each gene encoded in a genome, were reconstructed for each of the newly sequenced *Penicillium* species. Additional phylomes were reconstructed starting from *P. expansum* and *P. flavigenum*. All phylomes were reconstructed using a set of 33 species which included, which included our 10 *Penicillium* species, 20 additional *Penicillium* species and three outgroups: *Aspergillus clavatus, Talaromyces stipitatus* and *Emericella nidulans*. The annotated genomes for the three outgroups, as well as the other *Penicillium* genomes were retrieved from the NCBI genome database (https://www.ncbi.nlm.nih.gov/genome/ accessed on 20/12/2023), choosing species that at the beginning of study presented publicly available gene annotation (Suppl Table 2). Each phylome was reconstructed using the method described previously (Huerta-Cepas et al., 2011). Shortly, for each gene encoded in the genome of interest, in this case one of the newly sequenced *Penicillium* species, a blastP search was performed against the proteome database. Blast results were filtered, keeping only hits that had an e-value below 1e-05 and a contiguous homologous overlap covering at least 50% of the query sequence. For tree reconstruction, blast results were filtered to keep the best 150 hits. Sequences were then aligned using three different multiple sequence alignment programs (MUSCLE v3.8.31 (Edgar, 2004), MAFFT v6.814 b (Katoh et al., 2005) and KALIGN v2.4 (Lassmann and Sonnhammer, 2005) in both, forward and reverse (Landan and Graur, 2007). The resulting six alignments were then combined using M-coffee (T-Coffee v8.80) (Wallace et al., 2006). Trimming of the alignments was done with TrimAl v1.3 (Capella-Gutiérrez et al., 2009) (consistency cut-off of 0.1667, a gap score cutoff of 0.1 and a conservation score of 30%). Phylogenetic trees were reconstructed using a Neighbour Joining approach as implemented in BioNJ (Gascuel 1997). The likelihood of this topology was computed, allowing branch-length optimization, using seven different models (JTT, WAG, MtREV, VT, LG, Blosum62, and DCMut), as implemented in PhyML 3.0 (Guindon et al., 2010). The best model was selected according to the AIC criterion. A maximum likelihood tree was then derived using the selected model. In all cases a discrete gamma-distribution model with four rate categories plus invariant positions was used, the gamma parameter and the fraction of invariant positions were estimated from the data. Phylomes were stored in phylomeDB (https://phylomedb.org) (Fuentes et al., 2022) with phylomeIDs from 391 to 402. A cladogram was obtained using duptree (Wehe et al., 2008). Phylome 391 was scanned for the presence of trees that contained one single sequence per species. The alignments that resulted in these trees were concatenated into a single multiple sequence alignment. This alignment was then trimmed to eliminate positions of more than 20% gaps. The final alignment contained 786013 positions. IQTREE v1.6 (Nguyen et al., 2015) was then used to reconstruct the species tree using the LG + F + R6 model. 1000 ultrafast bootstraps were calculated and ETE3 was used to visualize the tree. Orthology relationships between different species were obtained using the species-overlap algorithm as implemented in ETE3 (Huerta-Cepas et al., 2016).

2.7. Chemical analyses

Secondary metabolites were extracted from fungal mycelium according to previously published protocols (Visagie et al., 2014). For both CYA and YES culture media, three biological replicates were prepared for each strain. Five plugs (5 mm-diameter) per medium pooled in one vial. Two technical replicas were obtained for each biological replication. The extractions of secondary metabolites were performed with a solution of ethyl acetate/dichloromethane/methanol (3:2:1) (v/v/v) with formic acid 1% (v/v). In details, 10 ml of solution were added to each sample and then sonication was carried out for 30 min at 25 °C. The supernatant was collected in a flask and the extraction operation was repeated a second time. The extract was evaporated through a rotary evaporator Laborota 4000-efficient (Heidolph Instruments, Germany), brought back into solution by adding 1 ml of methanol with formic acid 0.1% (v/v) and sonicated. The extracts were filtered through a Clarify-PP 0.22 μm polypropylene filter (Agela Technologies, China), and transferred into a HPLC vial for HPLC-DAD and LC-MS/MS analyses. Mycotoxins standards and HPLC and LC-MS purity grade solvents and reagents for chromatographic analyses were purchased from Sigma Aldrich (St. Louis, MO, USA).

Identification of the individual mycotoxins was performed by HPLC-DAD and LC-MS/MS. The HPLC-DAD chromatographic runs were

performed on a high-performance liquid chromatograph Agilent 1100 series (Agilent Technologies, Santa Clara, CA) which consists in an Agilent 1100 series quaternary pump coupled to an Agilent 1100 series Diode-Array Detector (DAD) and an Agilent 1100 series autosampler equipped with a 20 μL loop. The analyzes were carried out by monitoring five wavelengths (330, 300, 280, 254 and 228 nm). UV spectra of analyzes compounds are presented in Suppl Fig.1. The chromatography column was a Synergi 4 μm Hydro-RP (250 × 4.6 mm L. x I.D., 80 Å, Phenomenex, Torrance, CA, USA) under a flow rate of 1.0 mL/min. Solvent A was water (H_2O) and solvent B was methanol (MeOH), both acidified with formic acid 0.1% (v/v). Elution gradient started with 0% of solvent B, increased to 20% in 5 min, increased to 50% in 15 min and remained at 50% for 5 min. After, increased to 100% in 15 min and remained at 100% for 20 min, then decreased to 0% in 3 min and, finally, remained to 0% for 5 min. During the next 5 min, the column was washed and readjusted to the initial conditions and equilibrated for 10 min. The volume of the injection was 20 μL.

The LC-MS/MS system was a 1260 Agilent Technologies consisting of a binary pump and a vacuum degasser, connected to a Varian autosampler, Model 410 Prostar (Hansen Way, CA, USA), equipped with a 20 μL loop coupled to a Varian 310-MS TQ Mass Spectrometer. The mycotoxins were separated following previously reported methods (Spadaro et al., 2020), with minor modifications. The chromatography column was a Gemini 3 μm NX-C18 (150 × 3.0 mm L. x I.D., 110 Å, Phenomenex, Torrance, CA, USA) under a flow rate of 0.2 mL/min. Solvent A was H_2O acidified with formic acid 0.05% (v/v), while solvent B was acetonitrile (CH_3CN). Elution gradient started with 30% of solvent B for 5 min, increased to 50% in 10 min and remained at 50% for 10 min, then increased to 100% in 20 min. During the next 6 min, the column was washed and readjusted to the initial conditions and equilibrated for 10 min. The volume of the injection was 20 μL. The mass spectrometer was set to detect the positive and negative ion modes in different segments using an electrospray (ESI) ion source. The analysis was performed with following settings: drying temperature, 300 °C; needle voltage, 5 kV; capillary voltage, 80 V; drying gas pressure (nitrogen, N_2), 19 psi, and nebulizer gas pressure (air), 30 psi. For the multiple reaction monitoring (MRM) experiments, two transitions were selected for each compound (Suppl Table 3) and the collision gas (argon, Ar) pressure was set at 2 mbar for all the experiments. Collision energy is pivotal for orchestrating controlled molecular fragmentation, thereby augmenting the specificity and sensitivity of analysis. Through the regulation of ion collision kinetics, it becomes possible to obtain intricate details regarding the molecular structure and composition of analytes. Extracted-ion chromatogram (EIC) of considered mycotoxins and total ion current (TIC) chromatogram of the six mycotoxins standards are presented in Suppl Fig. 2 and Suppl Fig. 3, respectively.

2.8. Secondary metabolites (SM) selection

About 20 SMs were initially considered for analysis (Table 2), based on literature data and results of production assays in *Penicillium* spp. Reference protein sequences for associated BGCs were retrieved from the NCBI protein database (https://www.ncbi.nlm.nih.gov/protein/ accessed on 20/12/2023), using records from the Swiss-Prot database (The UniProt Consortium, 2019) where possible. In total, sequences associated to 17 SMs were found (Table 2), while the remaining three lacked any clustering data. These sequences were then used as query for a blastp search against the ten newly annotated proteomes. A BGC was considered as present in a strain genome if at least half of its proteins, including any synthase(s), aligned with a sequence identity higher than 65% to proteins in the target proteome. This resulted in seven SMs being discarded, with the other nine metabolites (five of which with

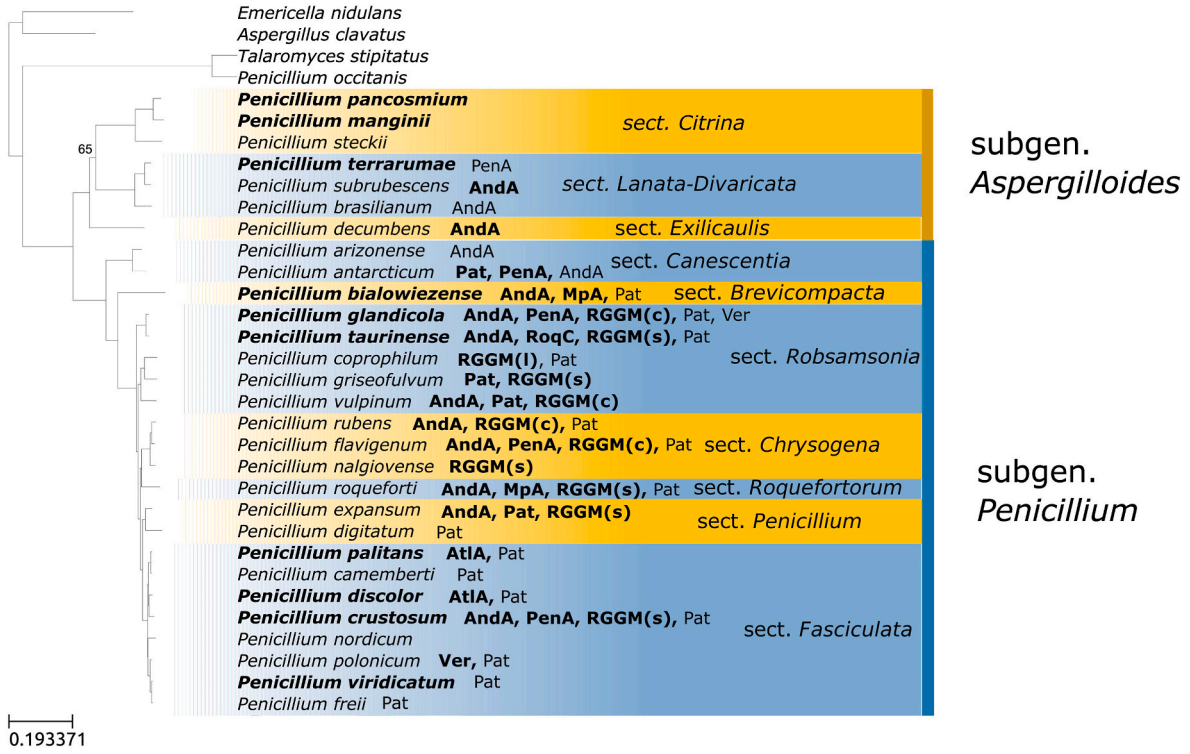

Fig. 1. Phylogenetic tree of studied *Penicillium* spp. Based on the concatenated alignment of 1301 single copy genes. Bootstrap support in all nodes is of 100 unless indicated. *Aspergillus clavatus*, *Emericella nidulans* and *Talaromyces stipitatus* were used as outgroups. In bold letters are species sequenced in thits study. For each species, the identified biosyntethic gene clusters are reported, with known production (either in literature or from our chemical analyses) indicated in bold. AndA: andrastin A cluster; AtlA: atlantinone A cluster; MpA: mycophenolic acid cluster; Pat: patulin cluster; PenA: penitrem A cluster; RGGM(c): roquefortine C – glandicoline A -glandicoline B – meleagrin cluster, complete form; RGGM(s): roquefortine C – glandicoline A -glandicoline B – meleagrin cluster, short form; Ver: verrucosidin.

mycotoxigenic potential), forming the final study pool of six BGCs (Table 2).

2.9. Phylome mining

Phylomes were reconstructed for each of the newly sequenced species to obtain reliable gene orthology relationships among *Penicillium* species. Phylome results were analyzed for genes encoded in each BGC at a time using the tools of the BLAST suite (Camacho et al., 2008) and python custom scripts. For each of the six BGCs a "seed" species was selected among the core species, based on mycotoxin production and preliminary blastp results. Protein codes for all putative BGC proteins in the "seed" species were retrieved and used for mining the phylome orthology data. Sequences of putative orthologs in "non-seed" species were retrieved and compared to the reference BGC proteins. In addition, they were aligned to the relevant genome to determine the position of their coding sequences. Reference BGC proteins sequences were also aligned directly against each "non-seed" species proteome and its corresponding genomic sequence, which reduced the impact of fusion proteins/incomplete "seed" species BGCs, and faulty gene prediction, respectively. Presence of BGCs inside "non-seed" species was identified based on composition and distribution of the orthologous proteins' coding sequences, as well as their identity value when compared to reference BGC proteins. An identity value cutoff was set at 65% for protein-protein alignments and at 80% for protein – translated nucleotide alignments. For the andrastin A cluster proteins a lower cutoff value of 55% was selected due to higher sequence heterogeneity, while tblastN values were lowered to 65%.

Table 4
Number of putative orthologs found for each BGC in each phylome species. Species highlighted in light grey were sequenced and annotated in this study. For each species, clusters associated with metabolite production are highlighted in green.

Species	Andrastin A	Mycophenolic acid	Patulin	Penitrem A	Roquefortine / Glandicoline A / Glandicoline B / Meleagrin	Verrucosidin
	N° of putative orthologs found/N° of genes in reference cluster					
Aspergillus clavatus	0/10	0/7	15/15	0/20	0/7	0/10
Emericella nidulans	0/10	0/7	0/15	0/20	0/7	0/10
Penicillium antarcticum	7/10	0/7	15/15	20/20	0/7	0/10
Penicillium arizonense	7/10	0/7	0/15	0/20	0/7	0/10
Penicillium bialowiezense	10/10	7/7	8/15	0/20	0/7	0/10
Penicillium brasilianum	6/10	0/7	0/15	0/20	0/7	0/10
Penicillium camemberti	7/10	0/7	7/15	0/20	0/7	0/10
Penicillium coprophilum	0/10	0/7	7/15	0/20	7/7	0/10
Penicillium crustosum	10/10	0/7	7/15	20/20	3/7	0/10
Penicillium decumbens	10/10	0/7	0/15	0/20	0/7	0/10
Penicillium digitatum	0/10	0/7	5/15	0/20	0/7	0/10
Penicillium discolor	7/10*	0/7	7/15	0/20	0/7	0/10
Penicillium expansum	10/10	0/7	15/15	0/20	3/7	0/10
Penicillium flavigenum	10/10	0/7	6/15	20/20	7/7	0/10
Penicillium freii	0/10	0/7	7/15	0/20	0/7	0/10
Penicillium glandicola	10/10	0/7	3/15	20/20	7/7	8/10
Penicillium griseofulvum	0/10	0/7	15/15	0/20	5/7	0/10
Penicillium manginii	0/10	0/7	0/15	0/20	0/7	0/10
Penicillium nalgiovense	0/10	0/7	0/15	0/20	3/7	0/10
Penicillium nordicum	0/10	0/7	0/15	0/20	0/7	0/10
Penicillium occitanis	0/10	0/7	0/15	0/20	0/7	0/10
Penicillium palitans	7/10*	0/7	7/15	0/20	0/7	0/10
Penicillium pancosmium	0/10	0/7	0/15	0/20	0/7	0/10
Penicillium polonicum	0/10	0/7	7/15	0/20	0/7	10/10
Penicillium roqueforti	10/10	7/7	11/15	0/20	3/7	0/10
Penicillium rubens	10/10	0/7	6/15	0/20	7/7	0/10
Penicillium steckii	0/10	0/7	0/15	0/20	0/7	0/10
Penicillium subrubescens	10/10	0/7	0/15	0/20	0/7	0/10
Penicillium taurinense	10/10	0/7	3/15	0/20	4/7	0/10
Penicillium terrarumae	0/10	0/7	0/15	5/20	0/7	0/10
Penicillium viridicatum	0/10	0/7	7/15	0/20	0/7	0/10
Penicillium vulpinum	10/10	0/7	15/15	0/20	7/7	0/10
Talaromyces stipitatus	0/10	0/7	0/15	0/20	0/7	0/10

* For *P. discolor* and *P. palitans* the partial andrastin A BGC was identified as an atlantinone A BGC.

3. Results and discussion

3.1. Genome sequencing and comparative genomics

The genome assembly statistics of *P. discolor*, *P. glandicola*, *P. crustosum, P. bialowiezense*, *P. pancosmium, P. palitans, P. viridicatum, P. manginii, P. terrarumae* and *P. taurinense* are presented in Table 1. Overall, assembly sizes ranged from 27.5 to 36.8 Mb and the number of encoded genes ranged from 9,867 to 12,520, with an average GC content of 48.6%. The number of Ns predicted in *P. discolor* (373.67 N per 100 kbp) was much higher than what was predicted for the other species (maximum 2.6 N per kbp). However, the number of predicted genes remained very similar to what was observed in the other genomes. Therefore, it is likely that the gene prediction, and the consequent secondary metabolite cluster analysis, were not affected by this limitation in the *P. discolor* assembly.

We used Antismash version 5.2.0 (Blin et al., 2019) to predict the presence of BGCs inside these species (Table 3). The total number of predicted BGCs is 551. BGC presence is quite variable in the different species, with *P. viridicatum* having almost twice the number of clusters of *P. pancosmium* (73 versus 38). The most represented families of core biosynthetic enzymes are non-ribosomal peptide synthases (NRPSs: 191)

Fig. 2. Structure of putative andrastin A clusters found in investigated *Penicillium* spp. Each line name indicates the species, while arrows indicate relative size and orientation of present genes, with the same color indicating homologues across different species. White arrows indicate genes not associated with known cluster genes. (For interpretation of the references to color in this figure legend, the reader is referred to the Web version of this article.)

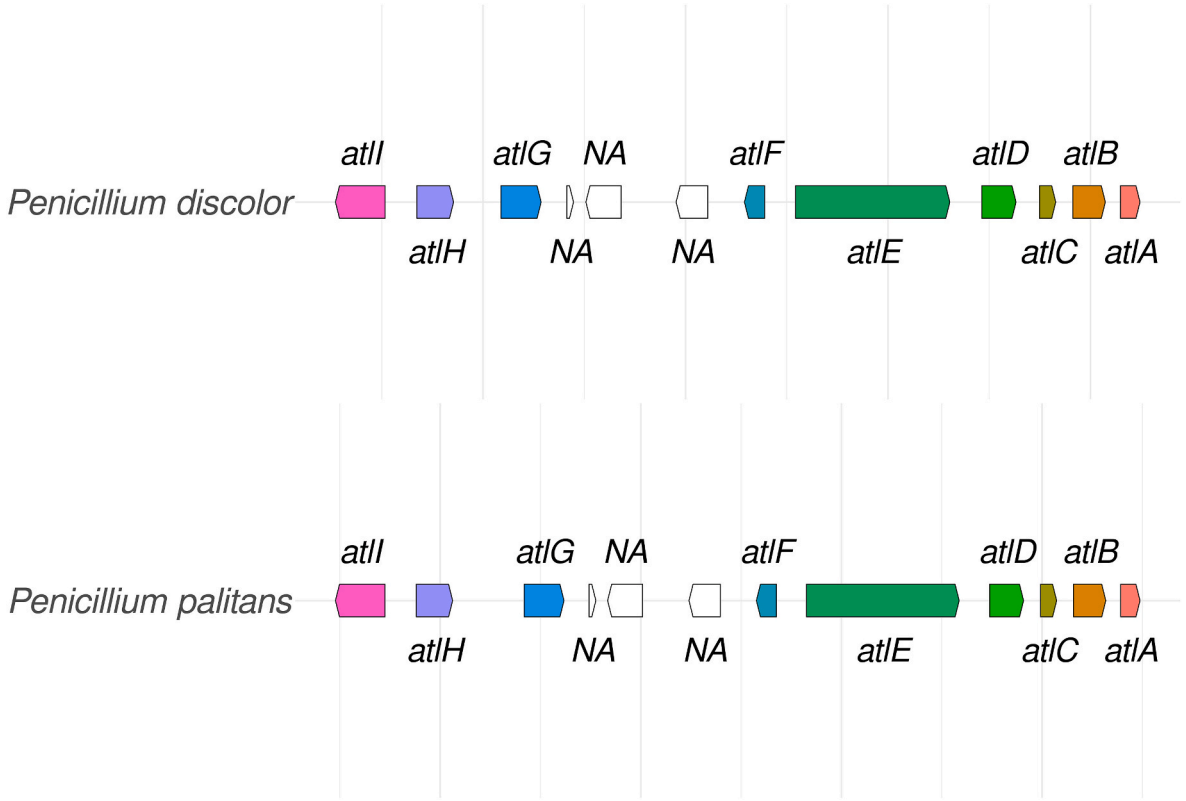

Fig. 3. Structure of putative atlantinone A clusters found in *P. discolor* and *P. palitans*. Each line name indicates the species, while arrows indicate relative size and orientation of present genes, with the same color indicating homologues across different genomes. White arrows indicate genes not associated with known cluster genes. (For interpretation of the references to color in this figure legend, the reader is referred to the Web version of this article.)

Fig. 4. Structure of putative mycophenolic acid clusters found in investigated *Penicillium* spp. Each line name indicates the species, while arrows indicate relative size and orientation of present genes, with the same color indicating homologues across different genomes. White arrows indicate genes not associated with known cluster genes. (For interpretation of the references to color in this figure legend, the reader is referred to the Web version of this article.)

and polyketide synthases (PKSs: 175), followed by terpene synthases (87), hybrid PKS-NRPSs (80) and dimethylallyltryptophan synthases (DMATSs: 15). Uncommon gene clusters include a ribosomally synthesized and post-translationally modified peptide (RiPP) cluster, found in *P. terrarumae, P. pancosmium* and *P. viridicatum*, and a siderophore cluster found in *P. manginii*.

We then reconstructed the phylogenetic relationships between these species and other sequenced *Penicillium* species (Fig. 1). Recently, a thorough taxonomical reassessment of the *Eurotiales* order has been performed based on nine loci (*BenA*, *CaM*, *Cct8*, *ITS*, *LSU*, *RPB1*, *RPB2*, *SSU* and *Tsr1*), with additional analyses of series relationships in *Aspergillus* and *Penicillium* genus (Houbraken et al., 2020). For the *Penicillium* genus, the overall topology obtained in our phylogenetic tree is similar to the one presented in the aforementioned study, for the species shared by both studies. However, in our reconstruction the divergence between sections *Brevicompacta* and *Canescentia* (both belonging to *Penicillium* subgenus *Penicillium*) occurred sequentially during the evolution of *Penicillium* subgenus *Penicillium*, with section *Canescentia* diverging before section *Brevicompacta*, whereas in Houbraken et al. (2020) these sections emerge together from a common ancestor. In our tree, *Penicillium occitanis* clustered with *Talaromyces stipitatus*, as shown in a previous study (Fuentes et al., 2022).

3.2. Biosynthetic gene clusters

Biosynthetic gene clusters (BGCs) are the genomic structures by which fungi organize and regulate the synthesis of secondary metabolites. In the present study, we used the knowledge of gene homology relationships to investigate the presence and completeness of some previously identified BGCs among several *Penicillium* species. In addition, for the newly sequenced strains, LC-MS/MS chemical analyses were performed for the production of the BGCs products in different growth media. Results of BGC analyses, under the tested conditions, are shown in Table 4. Overall, the highest number of putatively functioning BGCs (four) was found in *P. glandicola* and *P. roqueforti*. Four other species (*P. crustosum, P. vulpinum, P. flavigenum* and *P. expansum*) had three functioning clusters. *P. bialowiezense, P. taurinense, P. antarcticum, P. rubens* and *P griseofulvum* had two functioning clusters, whereas *P. decumbens, P. subrubescens, P. coprophilum, P. nalgiovense, P. discolor* and *P. palitans* had one functioning cluster. Finally, no putatively functioning cluster for the considered secondary metabolites was found in the remaining species.

3.2.1. Andrastin A and atlantinone A

Andrastin A cluster is formed by eleven genes, nine of which encode for enzymes which are directly involved in andrastin A formation: *adrA, adrD, adrE, adrF, adrG, adrH, adrI, adrJ* and *adrK* (Matsuda et al., 2013).

The andrastin A cluster was found in eleven *Penicillium* spp. (Fig. 2, Suppl Table 4), nine of which belong to *Penicillium* subgenus *Penicillium*.

While production of andrastin A has been previously reported in most of these species (Sonjak et al., 2005; Houbraken et al., 2012, Mansouri et al., 2013; Grijseels et al., 2017; Olsen et al., 2017; Prencipe et al., 2018; Olsen et al., 2019; Houbraken et al., 2020; Spadaro et al., 2020), we found no reference for its production by *P. taurinense* and *P. flavigenum*, which could be attributed to the species novelty (the former) or the presence of a silent cluster (the latter). Chemical analyses performed in this study confirmed these results for *P. bialowiezense, P. crustosum, P. glandicola,* and showed for the first time that *P. taurinense* can produce andrastin A (Suppl Fig. 4; Suppl Fig. 5; Suppl Fig. 6; Suppl Fig. 13). However, although we could identify the presence of this cluster in the genome of *P. flavigenum*, this species was unable to produce andrastin An under the tested conditions.

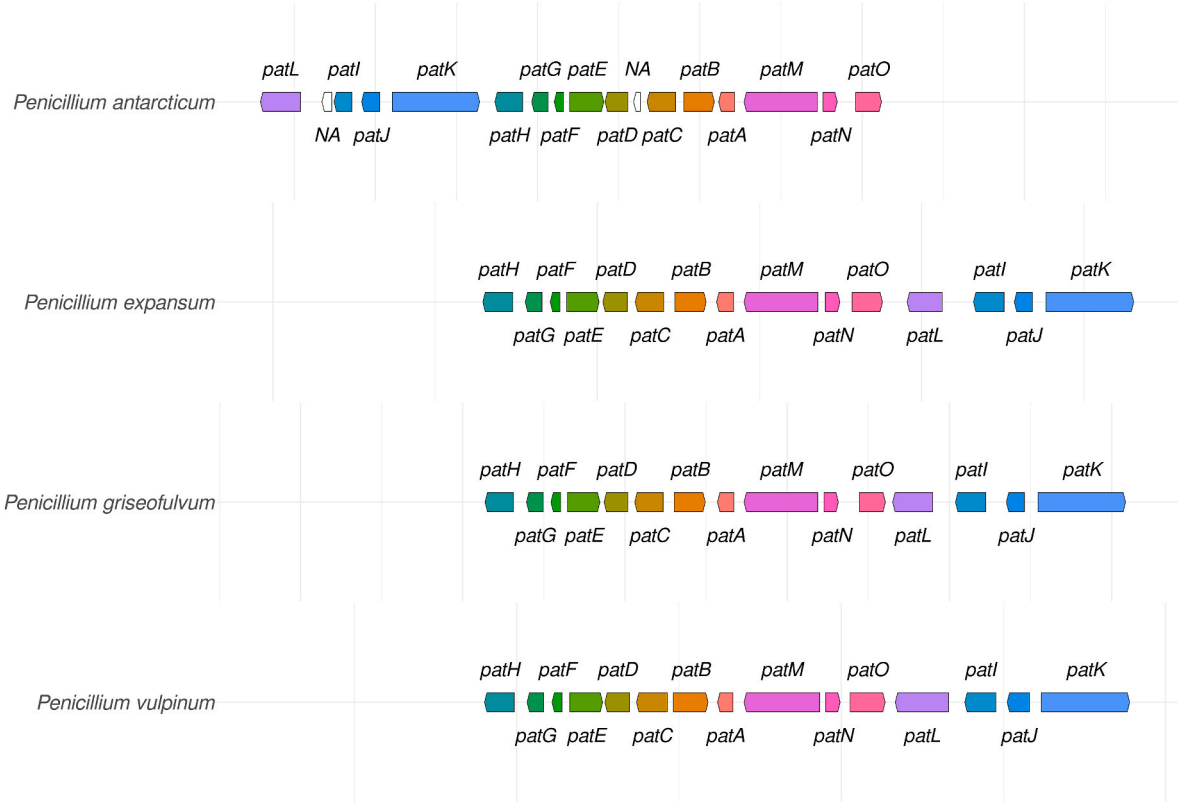

Fig. 5. Structure of putative complete patulin clusters found in investigated *Penicillium* spp. Each line name indicates the species, while arrows indicate size and orientation of present genes, with the same color indicating homologues across different genomes. White arrows indicate genes not associated with known cluster genes. Double lines indicate that genes are found in different contigs. (For interpretation of the references to color in this figure legend, the reader is referred to the Web version of this article.)

In addition to previous results, six more species seem to present homologues of the complete BGC, both from *Penicillium* subgenus *Penicillium* and *Penicillium* subgenus *Aspergilloides*: *P. antarcticum* (section *Canescentia*), *P. brasilianum* (section *Lanata-Divaricata*), *P. arizonense* (section *Canescentia*), *P. discolor, P. palitans* and *P. camemberti* (section *Fasciculata*). No andrastin A production has so far been observed in those species, although *P. discolor*, *P. palitans* and *P. anctarticum* are known to produce atlantinone A (Dalsgaard et al., 2012; Visagie et al., 2021) which shares the same initial intermediates, but diverges in later steps (Qi et al., 2022). Indeed, closer inspection of putative andrastin A BGC elements in *P. discolor* and *P. palitans* revealed the presence of a complete atlantinone A cluster (Fig. 3; Suppl Table 5). Our chemical analyses (Suppl Fig. 9; Suppl Fig. 11) later confirmed the production of atlantinone A in both *P. discolor* and *P. palitans*. Note that the complete biosynthetic pathway associated with the cluster allows the conversion of atlantinone A to hydroxylated derivate atlantinone B (Qi et al., 2022), which was not investigated in our study.

Although the remaining clusters could be explained as degenerated andrastin A or atlantinone A clusters, they might also represent parts of clusters whose proteins are responsible for the synthesis of related secondary metabolites. Indeed, apart from andrastin A and atlantinone A, many molecules of this family, which also includes mycophenolic acid, have been found in various Penicillium species, such as citreobybridones (Kosemura, 2003), penisemplicins (Komai et al., 2005), berkeleyacetals and berkeleyacetals-derivates (Stierle et al., 2011; Ren et al., 2019), purpurogenolide (Sun et al., 2016), simpterpenoid A (Li et al., 2018), austinol and austinol-derivates (Park et al., 2018) and brasilianoids (Zhang et al., 2018). For example, one of these molecules, paraherquonin, is produced in *P. brasilianum* strain NBRC 6234, where the associated BGC was also characterized (Matsuda et al., 2016).

3.2.2. Mycophenolic acid

The mycophenolic acid gene cluster is formed by seven genes, of which five encode for enzymes that are directly involved in mycophenolic acid formation: *mpaA, mpaC, mpaDE, mpaF* and *mpaG* (Regueira et al., 2011; Hansen et al., 2012; Zhang et al., 2015, 2019; Del-Cid et al., 2016), while the seventh and final gene, *mpaB*, seems to play a role in the pathway, although its function is unknown.

The mycophenolic acid cluster was found in two species from the *Penicillium* subgenus *Penicillium* (Fig. 4, Suppl Table 6): *P. bialowiezense* (section *Brevicompacta*), a very close relative of well-known mycophenolic acid producer *P. brevicompatum* (which is also part of section *Brevicompacta*, series *Brevicompacta)* (Houbraken et al., 2020) and *P. roqueforti* (section *Roquefortorum*) for which the production of the compound had been previously reported (Prencipe et al., 2018; Olsen et al., 2019; Kozlovsky et al., 2020; Spadaro et al., 2020). We here confirm that our strain of P. *bialowiezense* is also able to produce mycophenolic acid (Suppl Fig. 4).

3.2.3. Patulin

The patulin gene cluster is formed by fifteen genes, ten of which encode for enzymes which are known to be directly involved in the synthesis of patulin: *patD, patE, patF, patG, patH, patI, patJ, patK, patN* and *patO* (Beck et al., 1990; Dombrink-Kurtzman, 2007; Artigot et al., 2009; Snini et al., 2014; Tannous et al., 2017; Li et al., 2019). Three additional genes, *patA*, *patC* and *patM*, codify for putative transporters (Li et al., 2019). A fourteenth gene, *patL*, encodes for a transcription factor (Li et al., 2015), while the fifteenth gene, *patB*, encodes for a carboxysterase of unknown function. The patulin cluster was found in the outgroup *A. clavatus* and four *Penicillium* spp., all from *Penicillium* subgenus *Penicillium* (Fig. 5, Suppl Table 7): *P. antarcticum* (section *Canescentia*), *P. vulpinum, P. griseofulvum* (both section *Robsamsonia*), and *P. expansum* (section *Penicillium*). Production of this mycotoxin was

Fig. 6. Structure of putative patulin clusters found in investigated *Penicillium* spp. Each line name indicates the species, while arrows indicate size and orientation of present genes, with the same color indicating homologues across different genomes. White arrows indicate genes not associated with known cluster genes. (For interpretation of the references to color in this figure legend, the reader is referred to the Web version of this article.)

previously reported for all five of the species identified as having the gene cluster (Frisvad et al., 2004; Vansteelandt et al., 2012; Banani et al., 2016; Grijseels et al., 2017; Botha et al., 2018; Misihairabgwi et al., 2018; Spadaro et al., 2020; Visagie et al., 2021).

In addition, fifteen more species seem to present elements of the complete BGC, all from *Penicillium* subgenus *Penicillium* (Figs. 6 and 7, Suppl Table 7). Though none of the species has been previously reported as a patulin producer, we checked whether they could produce intermediate compounds of this pathway.

Based on gene composition, as well as identity values compared to reference proteins, it is possible to delineate three BGCs subgroups. The first subgroup (Fig. 6), formed by *P. coprophilum, P. roqueforti, P. flavigenum* and *P. rubens*, contains orthologs with high protein identity values (above 80%) that are continuous in the biosynthetic pathway and thus could result at least in the formation of intermediate products. Such occurrence has been previously observed in *P. coprophilum* and *P. flavigenum* (Nielsen et al., 2017), where isoepoxydon was produced, but the same study did not detect any patulin-related product in *P. rubens* and *P. roqueforti*. Production of isoepoxydon requires the presence of at least five genes: in order, *patK*, *patG*, *patH*, *patI* and *patJ*. All four species share these five genes, as well as *patL* (which encodes a transcription factor), in the same order, but there are differences in overall cluster structure. In particular, *P. flavigenum* and *P. rubens* patulin BGCs are identical and contain just the six aformentioned genes, though only the former is a patulin producer. *P. coprophilum*, the other isoepoxydon producer, presents two additional genes, *patC* (which encodes a putative transporter) and a gene of unknown function. Finally, *P. roqueforti* has the largest patulin BGC of the group, which also includes *patC*, *patM*, *patN* and *patO*, as well as three genes of unknown function. The second subgroup (Fig. 7), formed by *P. discolor, P. crustosum, P. palitans, P. camemberti, P. polonicum, P. freii* and *P. viridicatum*, contains orthologs with high protein identity values (above 90%) that do not form a biosynthetically continuous group. Since all these species belong to section *Fasciculata* and share the same cluster genes, it can be reasonably inferred that a patulin cluster was present and underwent degeneration in the common ancestor, and that the remaining cluster was inherited during the subsequent diversification of the section.

Finally, the third subgroup, formed by *P. bialowiezense, P. glandicola, P. digitatum* and *P. taurinense*, contains different orthologs with medium-to-high protein identity values (above 70%) that do not form a biosynthetically continuous group. For *P. digitatum* high protein identity values, as well as a close evolutionary relationship with patulin producing species *P. expansum* suggest degeneration of an ancestral patulin cluster. A similar hypothesis can be presented for *P. taurinense* based on high protein identity values, although closely related patulin producing species are unknown. These genes could also encode proteins responsible for the synthesis of related secondary metabolites, several of which have been detected in *Penicillium* spp. (Holm et al., 2014; Petersen et al., 2015; Tang et al., 2017). For *P. glandicola*, the presence of a limited number of genes associated with patulin production is puzzling, as this species has been previously reported to produce this molecule (Frisvad et al., 2004). Still, our production data (Suppl Table 7) confirm the absence of this mycotoxin, which point to the presence of these genes as leftovers after a cluster loss event rather than the result of a related BGC detection.

3.2.4. *Penitrem A*

Penitrem A cluster is formed by twenty genes, seventeen of which encode for enzymes which are directly involved in the synthesis of penitrem A: *ptmB, ptmC, ptmD, ptmE, ptmG, ptmH, ptmI, ptmJ, ptmK, ptmL, ptmM, ptmN, ptmO, ptmP, ptmQ, ptmU* and *ptmV* (Saikia et al., 2006; Liu et al., 2015). Two other genes, *ptmT* and *ptmS*, are thought to encode a

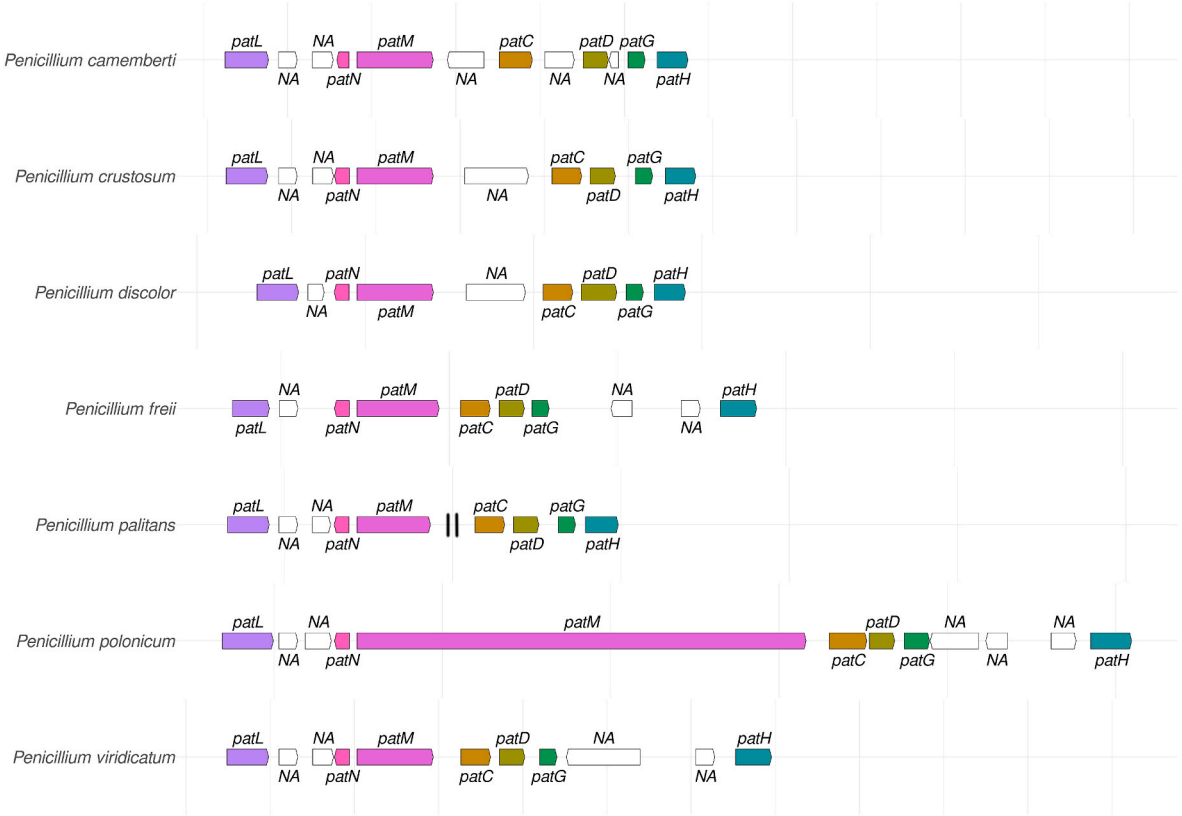

Fig. 7. Structure of putative patulin clusters found in investigated *Penicillium* spp. Each line name indicates the species, while arrows indicate size and orientation of present genes, with the same color indicating homologues across different genomes. White arrows indicate genes not associated with known cluster genes. Double lines indicate that genes are found in different contigs. (For interpretation of the references to color in this figure legend, the reader is referred to the Web version of this article.)

transporter and a transcription factor, respectively, while no role has been found for the product of gene *ptmA* (Liu et al., 2015).

A penitrem A cluster was found in four species, all from *Penicillium* subgenus *Penicillium* (Fig. 8, Suppl Table 8): *P. antarcticum* (section *Canescentia*), *P. glandicola* (section *Robsamsonia*), *P. flavigenum* (section *Chrysogena*) and *P. crustosum* (section *Fasciculata*), for all of which penitrem A production was reported (Overy et al., 2003; Frisvad et al., 2004; Kozlovsky et al., 2020; Visagie et al., 2021). Our chemical analyses (Suppl Fig. 5; Suppl Fig. 6) confirmed these results for *P. crustosum* and *P. glandicola*.

Another species, *P. terrarumae* (from *Penicillium* subgenus *Aspergilloides*, section *Lanata-Divaricata*), presents elements of the complete cluster with low-to-medium protein identity values (60–80 %) (Suppl Table 8). This could be the result of degeneration of an ancient penitrem cluster or, alternatively, it could indicate the presence of a related cluster producing similar metabolites, many of which have been detected in *Penicillium* spp. (Xu et al., 2007; Smetanina et al., 2007; Hu et al., 2017; Babu et al., 2018; Ariantari et al., 2019).

3.2.5. *Roquefortine C – glandicoline A – glandicoline B – meleagrin*

Roquefortine C/glandicoline A/glandicoline B/meleagrin (RGGM) cluster is formed by seven genes, six of them encoding for enzymes directly involved in the biosynthesis of these molecules: *roqA, roqD, roqM, roqN, roqO* and *roqR* (García-Estrada et al., 2011; Ali et al., 2013). A seventh gene, *roqT*, is thought to encode a transporter for extracellular secretion (García-Estrada et al., 2011).

A RGGM cluster was found in eleven species (all from *Penicillium* subgenus *Penicillium*), either in a complete configuration (responsible for the synthesis of roquefortine C, roquefortine D, roquefortine F, neoxaline, glandicoline A, glandicoline B and meleagrin) or a shortened one, yet still functional configuration (responsible just for the synthesis of roquefortine C) (Fig. 9, Suppl Table 9): for the complete configuration, *P. glandicola*, *P. vulpinum* and *P. coprophilum* (section *Robsamsonia*), *P. flavigenum* and *P. rubens* (section *Chrysogena*), whereas for the shortened configuration *P. taurinense* and *P. griseofulvum* (section *Robsamsonia*), *P. roqueforti* (section *Roquefortorum*), *P. nalgiovense* (section *Chrysogena*), *P. expansum* (section *Penicillium*) and *P. crustosum* (section *Fasciculata*).

For the complete configuration BGC all aforementioned species have been previously reported to produce both roquefortine C and meleagrin (Frisvad et al., 2004; Grijseels et al., 2017; Prencipe et al., 2018; Kozlovsky et al., 2020), while for the shortened configuration production of just roquefortine C was previously reported in all indicated species but *P. taurinense* and *P. nalgiovense* (Frisvad et al., 2004; Banani et al., 2016; Prencipe et al., 2018; Spadaro et al., 2020; Kozlovsky et al., 2020). In *P. nalgiovense*, the presence of a putatively inactive cluster residue was previously noted (Nielsen et al., 2017). Our chemical analyses (Suppl Fig. 5; Suppl Fig. 6; Suppl Fig. 13) provided evidence for roquefortine C production in *P. crustosum*, *P. glandicola* and *P. taurinense*, as well as glandicoline A, glandicoline B and meleagrin production in *P. glandicola*.

3.2.6. *Verrucosidin*

Verrucosidin cluster is thought to be formed by ten genes, of which one encodes for a polyketide synthase which is known to be directly involved in verrucosidin biosynthesis: *verA* (Valente et al., 2021). Genes *verB, verC1*, *verC2*, *verF*, *verG* and *verH* received a putative function, whereas the role of genes *verU1, verU2* and *verU3* remains unknown.

A verrucosidin cluster was found in two phylome species, both from *Penicillium* subgenus *Penicillium* (Fig. 10, Suppl Table 10): *P. polonicum* (section *Fasciculata*) had the complete cluster and *P. glandicola* (section *Robsamsonia*), with eight genes out of ten. Production of verrucosidin

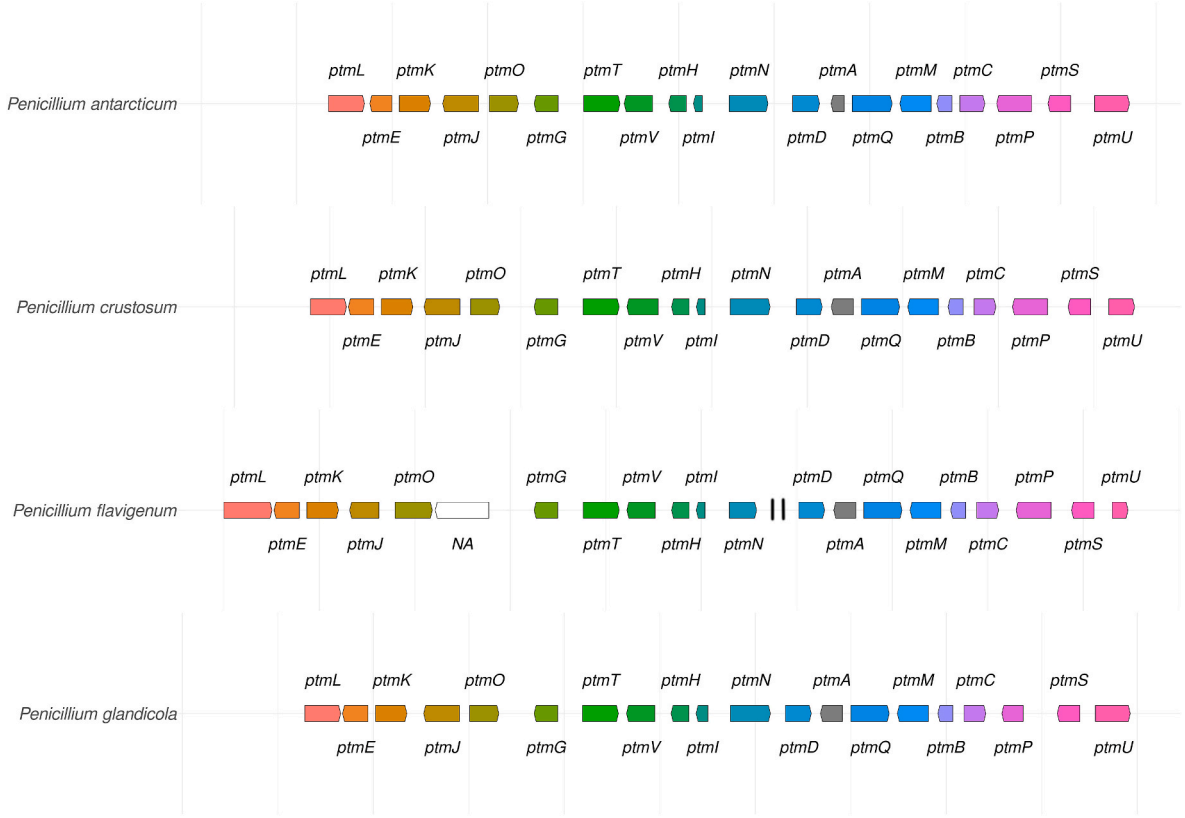

Fig. 8. Structure of putative penitrem A clusters found in investigated *Penicillium* spp. Each line name indicates the species, while arrows indicate relative size and orientation of present genes, with the same color indicating homologues across different genomes. White arrows indicate genes not associated with known cluster genes. Double lines indicate that genes are found in different contigs. (For interpretation of the references to color in this figure legend, the reader is referred to the Web version of this article.)

Fig. 9. Structure of putative roquefortine C/glandicoline A/glandicoline B/meleagrin clusters found in investigated *Penicillium* spp. Each line name indicates the species, while arrows indicate relative size and orientation of present genes, with the same color indicating homologues across different genomes. White arrows indicate genes not associated with known cluster genes. (For interpretation of the references to color in this figure legend, the reader is referred to the Web version of this article.)

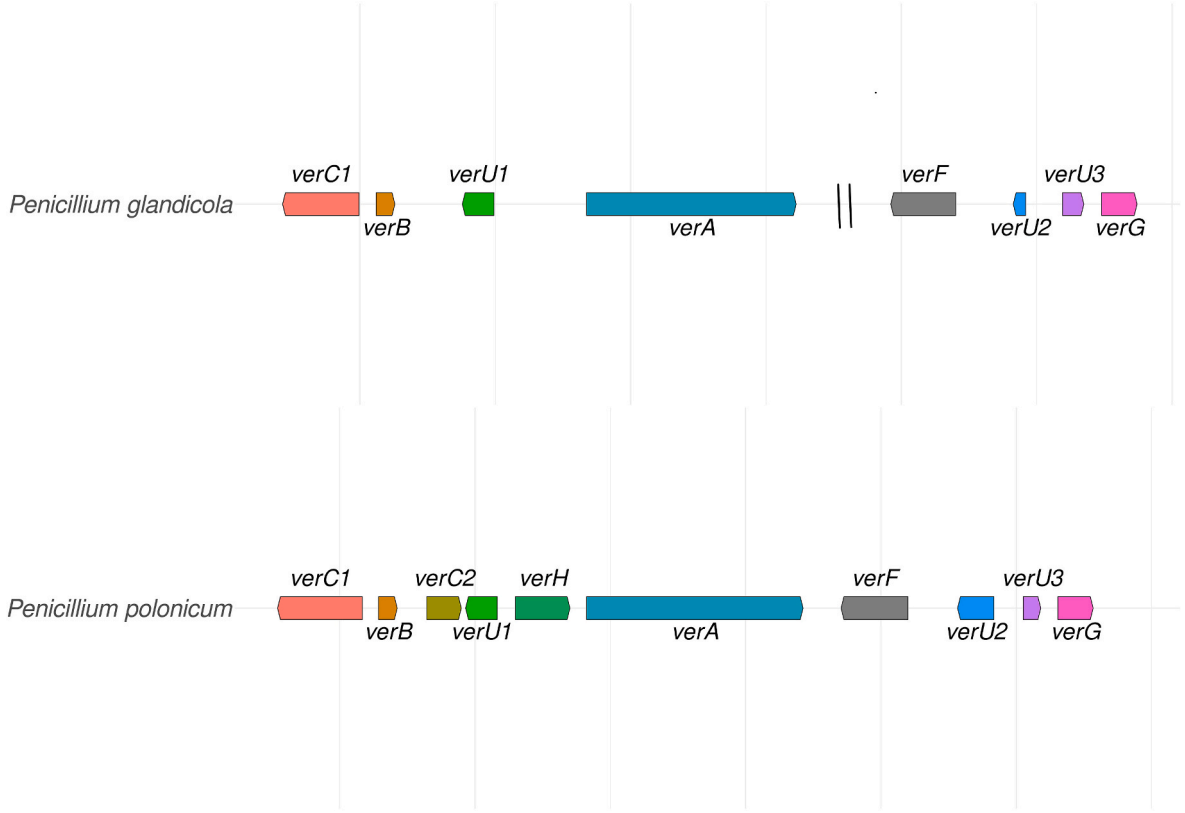

Fig. 10. Structure of putative verrucosidin clusters found in investigated *Penicillium* spp. Each line name indicates the species, while each arrow indicates relative size and orientation of present genes, with the same color indicating homologues across different genomes. White arrows indicate genes not associated with known cluster genes. Double lines indicate that genes are found in different contigs. (For interpretation of the references to color in this figure legend, the reader is referred to the Web version of this article.)

has been previously reported in *P. polonicum* (Frisvad et al., 2004; Wigmann et al., 2015). No literature data was found for verrucosidin production in *P. glandicola,* which is consistent with our results for this species, in which this cluster lacks the biosynthetic genes *verC2* and *verH*. Our chemical analyses (Suppl Fig. 6) confirmed the lack of verrucosidin production in our strain of *P. glandicola*.

4. Conclusions

In this study we sequenced and annotated ten *Penicillium* genomes belonging to section *Lanata-Divaricata* (*P. terrarumae*), section *Citrina* (*P. pancosmium* and *P. manginii*), section *Brevicompacta* (*P. bialowiezense*), section *Robsamsonia* (*P. glandicola* and *P. taurinense*) and section *Fasciculata* (*P. discolor*, *P. crustosum, P. palitans* and *P. viridicatum*), thus increasing the available information regarding this genus. In particular, *P. glandicola, P. taurinense* and *P. terrarumae* were sequenced for the first time. All the strains were isolated from chestnuts and the chestnut flour production line. Most of these species can produce mycotoxins, which can cause acute and/or chronic toxicity to humans. The presence of such a high concentration of different *Penicillium* species in a food production line suggests a potential for combined production of different secondary metabolites, and particularly of mycotoxins.

In this study, we investigated the distribution and composition of six BGCs associated with the production of mycotoxins and other secondary metabolites, in particular andrastin A, atlantinone A, mycophenolic acid, penitrem A, patulin, verrucosidin, roquefortine C, glandicoline A, glandicoline B and meleagrin. We were able to identify mycotoxin clusters in species that so-far had not been reported to produce them. We identified an andrastin A cluster both in *P. vulpinum* and *P. flavigenum*, as well as a roquefortine C cluster in *P. nalgiovense*, thus suggesting a greater mycotoxigenic potential than previously expected. We demonstrated that members of the same section can have different mycotoxin BGCs and production, as observed for *P. glandicola* and *P. taurinense*, belonging to the same section Robsamsonia. *P. glandicola* has the complete BGCs and production of andrastin A, penitrem A and meleagrin/glandicoline/roquefortine C. *P. taurinense* showed for the first time to have both the BGC and the production of andrastin A and roquefortine C, but not of penitrem A.

Chestnuts, besides proving to be an optimal substrate for *Penicillium* spp. growth, showed to host several species with different mycotoxin potential, opening the door to the risks related to the occurrence of multiple mycotoxins in the same food matrix. This study outlines that a systemic approach should be adopted to mycotoxin risk evaluation and management, as several mycotoxins can be present on the same food matrix or food production line.

This study clarifies the mycotoxigenic potential of 31 species of *Penicillium*, three of which (*P. glandicola, P. taurinense* and *P. terrarumae*) had not been previously sequenced. This knowledge could be used in different food matrices, besides nuts, to establish the mycotoxigenic potential of *Penicillium* spp.

Data availability statement

Genome assemblies and annotation data have been deposited in ENA (European Nucleotide Archive). Accession numbers are provided in the text.

CRediT authorship contribution statement

Marco Garello: Writing – review & editing, Writing – original draft, Visualization, Validation, Software, Methodology, Investigation, Formal analysis, Data curation, Conceptualization. **Edoardo Piombo:** Writing –

review & editing, Writing – original draft, Validation, Software, Methodology, Investigation, Formal analysis, Data curation, Conceptualization. **Fabio Buonsenso:** Writing – review & editing, Writing – original draft, Visualization, Validation, Methodology, Investigation, Formal analysis, Data curation. **Simona Prencipe:** Validation, Methodology, Investigation, Formal analysis, Data curation, Conceptualization, Writing – original draft, Writing – review & editing. **Silvia Valente:** Formal analysis, Investigation, Methodology, Validation, Writing - review & editing. **Giovanna Roberta Meloni:** Formal analysis, Investigation, Methodology, Validation, Writing - review & editing. **Marina Marcet-Houben:** Conceptualization, Data curation, Investigation, Methodology, Software, Validation, Writing – original draft. **Toni Gabaldón:** Conceptualization, Data curation, Funding acquisition, Methodology, Project administration, Resources, Software, Supervision, Validation, Writing – original draft, Writing – review & editing. **Davide Spadaro:** Writing – review & editing, Writing – original draft, Validation, Supervision, Software, Conceptualization, Data curation, Funding acquisition, Methodology, Project administration, Resources.

Declaration of competing interest

The authors declare that they have no known competing financial interests or personal relationships that could have appeared to influence the work reported in this paper.

Acknowledgements

Part of this work was granted by the European Commission – NextGenerationEU, Project "Strengthening the MIRRI Italian Research Infrastructure for Sustainable Bioscience and Bioeconomy", code n. IR0000005. TG group acknowledges support from the Spanish Ministry of Science and Innovation for grants PID2021-126067NB-I00, CPP2021-008552, PCI2022-135066-2, and PDC2022-133266-I00, cofounded by ERDF "A way of making Europe"; from the Catalan Research Agency (AGAUR) SGR01551; from the European Union's Horizon 2020 research and innovation program (ERC-2016-724173); from the Gordon and Betty Moore Foundation (Grant GBMF9742); from the "La Caixa" foundation (Grant LCF/PR/HR21/00737), and from the Instituto de Salud Carlos III (IMPACT Grant IMP/00019 and CIBERINFEC CB21/13/00061- ISCIII-SGEFI/ERDF).

Appendix A. Supplementary data

Supplementary data to this article can be found online at https://doi.org/10.1016/j.fm.2024.104532.

References

Abbas, A., Coghlan, A., O'Callaghan, J., García-Estrada, C., Martín, J.F., Dobson, A.D., 2013. Functional characterization of the polyketide synthase gene required for ochratoxin A biosynthesis in *Penicillium verrucosum*. Int. J. Food Microbiol. 161 (3), 172–181. https://doi.org/10.1016/j.ijfoodmicro.2012.12.014.

Ali, H., Ries, M.I., Nijland, J.G., Lankhorst, P.P., Hankemeier, T., Bovenberg, R.A., Vreeken, R.J., Driessen, A.J., 2013. A branched biosynthetic pathway is involved in production of roquefortine and related compounds in *Penicillium chrysogenum*. PLoS One 8 (6), e65328. https://doi.org/10.1371/journal.pone.0065328.

Ariantari, N.P., Ancheeva, E., Wang, C., Mándi, A., Knedel, T.O., Kurtán, T., Chaidir, C., Müller, W., Kassack, M.U., Janiak, C., Daletos, G., Proksch, P., 2019. Indole diterpenoids from an endophytic *Penicillium* sp. J. Nat. Prod. 82 (6), 1412–1423. https://doi.org/10.1021/acs.jnatprod.8b00723.

Arras, G., Dhallewin, G., Petretto, A., Marceddu, S., Loche, M., Agabbio, M., 2005. Biological and physical approaches to improve induced resistance against green mold of stored citrus fruit. Commun. Agric. Appl. Biol. Sci. 70 (3), 391–397.

Artigot, M.P., Loiseau, N., Laffitte, J., Mas-Reguieg, L., Tadrist, S., Oswald, I.P., Puel, O., 2009. Molecular cloning and functional characterization of two CYP619 cytochrome P450s involved in biosynthesis of patulin in *Aspergillus clavatus*. Microbiology (Reading, England) 155 (Pt 5), 1738–1747. https://doi.org/10.1099/mic.0.024836-0.

Babu, J.V., Popay, A.J., Miles, C.O., Wilkins, A.L., di Menna, M.E., Finch, S.C., 2018. Identification and structure elucidation of janthitrems A and D from *Penicillium janthinellum* and determination of the tremorgenic and anti-insect activity of janthitrems A and B. J. Agric. Food Chem. 66 (50), 13116–13125. https://doi.org/10.1021/acs.jafc.8b04964.

Banani, H., Marcet-Houben, M., Ballester, A.R., Abbruscato, P., González-Candelas, L., Gabaldón, T., Spadaro, D., 2016. Genome sequencing and secondary metabolism of the postharvest pathogen *Penicillium griseofulvum*. BMC Genom. 17, 19. https://doi.org/10.1186/s12864-015-2347-x.

Bankevich, A., Nurk, S., Antipov, D., Gurevich, A.A., Dvorkin, M., Kulikov, A.S., Lesin, V. M., Nikolenko, S.I., Pham, S., Prjibelski, A.D., Pyshkin, A.V., Sirotkin, A.V., Vyahhi, N., Tesler, G., Alekseyev, M.A., Pevzner, P.A., 2012. SPAdes: a new genome assembly algorithm and its applications to single-cell sequencing. J. Comput. Biol.: a journal of computational molecular cell biology 19 (5), 455–477. https://doi.org/10.1089/cmb.2012.0021.

Beck, J., Ripka, S., Siegner, A., Schiltz, E., Schweizer, E., 1990. The multifunctional 6-methylsalicylic acid synthase gene of *Penicillium patulum*. Its gene structure relative to that of other polyketide synthases. Eur. J. Biochem. 192 (2), 487–498.

Blin, K., Shaw, S., Steinke, K., Villebro, R., Ziemert, N., Lee, S.Y., Medema, M.H., Weber, T., 2019. antiSMASH 5.0: updates to the secondary metabolite genome mining pipeline. Nucleic Acids Res. 47 (W1), W81–W87. https://doi.org/10.1093/nar/gkz310.

Bolger, A.M., Lohse, M., Usadel, B., 2014. Trimmomatic: a flexible trimmer for Illumina sequence data. Bioinformatics 30 (15), 2114–2120. https://doi.org/10.1093/bioinformatics/btu170.

Botha, C.J., Truter, M., Sulyok, M., 2018. Multimycotoxin analysis of South African *Aspergillus clavatus* isolates. Mycotoxin Res. 34 (2), 91–97. https://doi.org/10.1007/s12550-017-0303-0.

Cabañes, F.J., Bragulat, M.R., Castellá, G., 2010. Ochratoxin A producing species in the genus *Penicillium*. Toxins 2 (5), 1111–1120. https://doi.org/10.3390/toxins2051111.

Camacho, C., Coulouris, G., Avagyan, V., Ma, N., Papadopoulos, J.B., Madden, T.L., 2008. BLAST+: architecture and applications. BMC Bioinf. 10, 421. https://doi.org/10.1186/1471-2105-10-421.

Campbell, M.S., Holt, C., Moore, B., Yandell, M., 2014. Genome annotation and curation using MAKER and MAKER-P. Current protocols in bioinformatics 48, 4.11.1–4.11.39. https://doi.org/10.1002/0471250953.bi0411s48.

Capella-Gutiérrez, S., Silla-Martínez, J.M., Gabaldón, T., 2009. trimAl: a tool for automated alignment trimming in large-scale phylogenetic analyses. Bioinformatics 25 (15), 1972–1973. https://doi.org/10.1093/bioinformatics/btp348.

Chang, P.K., Horn, B.W., Dorner, J.W., 2009. Clustered genes involved in cyclopiazonic acid production are next to the aflatoxin biosynthesis gene cluster in *Aspergillus flavus*. Fungal Genet. Biol.: FG & B 46 (2), 176–182. https://doi.org/10.1016/j.fgb.2008.11.002.

Cimermancic, P., Medema, M.H., Claesen, J., Kurita, K., Wieland Brown, L.C., Mavrommatis, K., Pati, A., Godfrey, P.A., Koehrsen, M., Clardy, J., Birren, B.W., Takano, E., Sali, A., Linington, R.G., Fischbach, M.A., 2014. Insights into secondary metabolism from a global analysis of prokaryotic biosynthetic gene clusters. Cell 158 (2), 412–421. https://doi.org/10.1016/j.cell.2014.06.034.

Crous, P.W., Wingfield, M.J., Chooi, Y.H., Gilchrist, C., Lacey, E., Pitt, J.I., Roets, F., Swart, W.J., Cano-Lira, J.F., Valenzuela-Lopez, N., Hubka, V., Shivas, R.G., Stchigel, A.M., Holdom, D.G., Jurjević, Ž., Kachalkin, A.V., Lebel, T., Lock, C., Martín, M.P., Tan, Y.P., et al., 2020. Fungal Planet description sheets: 1042-1111. Persoonia 44, 301–459. https://doi.org/10.3767/persoonia.2020.44.11.

Dalsgaard, P.W., Petersen, B.O., Duus, J.Ø., Zidorn, C., Frisvad, J.C., Christophersen, C., Larsen, T.O., 2012. Atlantinone A, a meroterpenoid produced by *Penicillium ribeum* and several cheese associated *Penicillium* species. Metabolites 2 (1), 214–220. https://doi.org/10.3390/metabo2010214.

Del-Cid, A., Gil-Durán, C., Vaca, I., Rojas-Aedo, J.F., García-Rico, R.O., Levicán, G., Chávez, R., 2016. Identification and functional analysis of the mycophenolic acid gene cluster of *Penicillium roqueforti*. PLoS One 11 (1), e0147047. https://doi.org/10.1371/journal.pone.0147047.

Dombrink-Kurtzman, M.A., 2007. The sequence of the isoepoxydon dehydrogenase gene of the patulin biosynthetic pathway in *Penicillium* species. Antonie Leeuwenhoek 91 (2), 179–189. https://doi.org/10.1007/s10482-006-9109-3.

Edgar, R.C., 2004. MUSCLE: a multiple sequence alignment method with reduced time and space complexity. BMC Bioinf. 5, 113. https://doi.org/10.1186/1471-2105-5-113.

Flynn, J.M., Hubley, R., Goubert, C., Rosen, J., Clark, A.G., Feschotte, C., Smit, A.F., 2020. RepeatModeler2 for automated genomic discovery of transposable element families. Proc. Natl. Acad. Sci. U.S.A. 117 (17), 9451–9457. https://doi.org/10.1073/pnas.1921046117.

Freire, F.D., da Rocha, M.E., 2016. Impact of mycotoxins on human health. In: Mérillon, J.M., Ramawat, K. (Eds.), Fungal Metabolites. Reference Series in Phytochemistry. Springer, Cham, pp. 1–23. https://doi.org/10.1007/978-3-319-19456-1_21-1.

Frisvad, J.C., Smedsgaard, J., Larsen, T.O., Samson, R.A., 2004. Mycotoxins, drugs and other extrolites produced by species in *Penicillium* subgenus *Penicillium*. Stud. Mycol. 49, 201–241.

Frisvad, J.C., 2015. Taxonomy, chemodiversity, and chemoconsistency of *Aspergillus, Penicillium*, and *Talaromyces* species. Front. Microbiol. 5, 773. https://doi.org/10.3389/fmicb.2014.00773.

Fuentes, D., Molina, M., Chorostecki, U., Capella-Gutiérrez, S., Marcet-Houben, M., Gabaldón, T., 2022. PhylomeDB V5: an expanding repository for genome-wide catalogues of annotated gene phylogenies. Nucleic Acids Res. 50 (D1), D1062–D1068. https://doi.org/10.1093/nar/gkab966.

García-Estrada, C., Ullán, R.V., Albillos, S.M., Fernández-Bodega, M.Á., Durek, P., von Döhren, H., Martín, J.F., 2011. A single cluster of coregulated genes encodes the biosynthesis of the mycotoxins roquefortine C and meleagrin in *Penicillium*

chrysogenum. Chem. Biol. 18 (11), 1499–1512. https://doi.org/10.1016/j.chembiol.2011.08.012.
Gascuel, O., 1997. BIONJ: an improved version of the NJ algorithm based on a simple model of sequence data. Mol. Biol. Evol. 14 (7), 685–695. https://doi.org/10.1093/oxfordjournals.molbev.a025808.
Geisen, R., Schmidt-Heydt, M., Karolewiez, A., 2006. A gene cluster of the ochratoxin A biosynthetic genes in *Penicillium*. Mycotoxin Res. 22 (2), 134–141. https://doi.org/10.1007/BF02956777.
Gil-Serna, J., García-Díaz, M., González-Jaén, M.T., Vázquez, C., Patiño, B., 2018. Description of an orthologous cluster of ochratoxin A biosynthetic genes in *Aspergillus* and *Penicillium* species. A comparative analysis. Int. J. Food Microbiol. 268, 35–43. https://doi.org/10.1016/j.ijfoodmicro.2017.12.028.
Grigoriev, I.V., Nikitin, R., Haridas, S., Kuo, A., Ohm, R., Otillar, R., Riley, R., Salamov, A., Zhao, X., Korzeniewski, F., Smirnova, T., Nordberg, H., Dubchak, I., Shabalov, I., 2014. MycoCosm portal: gearing up for 1000 fungal genomes. Nucleic Acids Res. 42 (Database issue), D699–D704. https://doi.org/10.1093/nar/gkt1183.
Grijseels, S., Nielsen, J.C., Nielsen, J., Larsen, T.O., Frisvad, J.C., Nielsen, K.F., Frandsen, R., Workman, M., 2017. Physiological characterization of secondary metabolite producing *Penicillium* cell factories. Fungal biology and biotechnology 4, 8. https://doi.org/10.1186/s40694-017-0036-z.
Guindon, S., Dufayard, J.F., Lefort, V., Anisimova, M., Hordijk, W., Gascuel, O., 2010. New algorithms and methods to estimate maximum-likelihood phylogenies: assessing the performance of PhyML 3.0. Syst. Biol. 59 (3), 307–321. https://doi.org/10.1093/sysbio/syq010.
Gurevich, A., Saveliev, V., Vyahhi, N., Tesler, G., 2013. QUAST: quality assessment tool for genome assemblies. Bioinformatics 29 (8), 1072–1075. https://doi.org/10.1093/bioinformatics/btt086.
Hansen, B.G., Mnich, E., Nielsen, K.F., Nielsen, J.B., Nielsen, M.T., Mortensen, U.H., Larsen, T.O., Patil, K.R., 2012. Involvement of a natural fusion of a cytochrome P450 and a hydrolase in mycophenolic acid biosynthesis. Appl. Environ. Microbiol. 78 (14), 4908–4913. https://doi.org/10.1128/AEM.07955-11.
Hoff, K.J., Stanke, M., 2013. WebAUGUSTUS–a web service for training AUGUSTUS and predicting genes in eukaryotes. Nucleic Acids Res. 41 (Web Server issue), W123–W128. https://doi.org/10.1093/nar/gkt418.
Holm, D.K., Petersen, L.M., Klitgaard, A., Knudsen, P.B., Jarczynska, Z.D., Nielsen, K.F., Gotfredsen, C.H., Larsen, T.O., Mortensen, U.H., 2014. Molecular and chemical characterization of the biosynthesis of the 6-MSA-derived meroterpenoid yanuthone D in *Aspergillus niger*. Chem. Biol. 21 (4), 519–529. https://doi.org/10.1016/j.chembiol.2014.01.013.
Houbraken, J., Frisvad, J.C., Seifert, K.A., Overy, D.P., Tuthill, D.M., Valdez, J.G., Samson, R.A., 2012. New penicillin-producing *Penicillium* species and an overview of section Chrysogena. Persoonia 29, 78–100. https://doi.org/10.3767/003158512X660571.
Houbraken, J., Kocsubé, S., Visagie, C.M., Yilmaz, N., Wang, X.C., Meijer, M., Kraak, B., Hubka, V., Bensch, K., Samson, R.A., Frisvad, J.C., 2020. Classification of *Aspergillus, Penicillium, Talaromyces* and related genera (*Eurotiales*): an overview of families, genera, subgenera, sections, series and species. Stud. Mycol. 95, 5–169. https://doi.org/10.1016/j.simyco.2020.05.002.
Hu, X.Y., Meng, L.H., Li, X., Yang, S.Q., Li, X.M., Wang, B.G., 2017. Three new indole diterpenoids from the sea-anemone-derived fungus *Penicillium* sp. AS-79. Mar. Drugs 15 (5), 137. https://doi.org/10.3390/md15050137.
Huerta-Cepas, J., Capella-Gutierrez, S., Pryszcz, L.P., Denisov, I., Kormes, D., Marcet-Houben, M., Gabaldón, T., 2011. PhylomeDB v3.0: an expanding repository of genome-wide collections of trees, alignments and phylogeny-based orthology and paralogy predictions. Nucleic Acids Res. 39 (Database issue), D556–D560. https://doi.org/10.1093/nar/gkq1109.
Huerta-Cepas, J., Serra, F., Bork, P., 2016. Ete 3: reconstruction, analysis, and visualization of phylogenomic data. Mol. Biol. Evol. 33 (6), 1635–1638. https://doi.org/10.1093/molbev/msw046.
Ishikawa, N., Tanaka, H., Koyama, F., Noguchi, H., Wang, C.C., Hotta, K., Watanabe, K., 2014. Non-heme dioxygenase catalyzes atypical oxidations of 6,7-bicyclic systems to form the 6,6-quinolone core of viridicatin-type fungal alkaloids. Angew. Chem. 53 (47), 12880–12884. https://doi.org/10.1002/anie.201407920.
Ishiuchi, K., Nakazawa, T., Yagishita, F., Mino, T., Noguchi, H., Hotta, K., Watanabe, K., 2013. Combinatorial generation of complexity by redox enzymes in the chaetoglobosin A biosynthesis. J. Am. Chem. Soc. 135 (19), 7371–7377. https://doi.org/10.1021/ja402828w.
Karolewiez, A., Geisen, R., 2004. Cloning a part of the ochratoxin A biosynthetic gene cluster of *Penicillium nordicum* and characterization of the ochratoxin polyketide synthase gene. Syst. Appl. Microbiol. 28 (7), 588–595. https://doi.org/10.1016/j.syapm.2005.03.008.
Kato, N., Tokuoka, M., Shinohara, Y., Kawatani, M., Uramoto, M., Seshime, Y., Fujii, I., Kitamoto, K., Takahashi, T., Takahashi, S., Koyama, Y., Osada, H., 2011. Genetic safeguard against mycotoxin cyclopiazonic acid production in *Aspergillus oryzae*. Chembiochem : a European journal of chemical biology 12 (9), 1376–1382. https://doi.org/10.1002/cbic.201000672.
Katoh, K., Kuma, K., Toh, H., Miyata, T., 2005. MAFFT version 5: improvement in accuracy of multiple sequence alignment. Nucleic Acids Res. 33 (2), 511–518. https://doi.org/10.1093/nar/gki198.
Keller, N.P., 2019. Fungal secondary metabolism: regulation, function and drug discovery. Nat. Rev. Microbiol. 17 (3), 167–180. https://doi.org/10.1038/s41579-018-0121-1.
Kishimoto, S., Hara, K., Hashimoto, H., Hirayama, Y., Champagne, P.A., Houk, K.N., Tang, Y., Watanabe, K., 2018. Enzymatic one-step ring contraction for quinolone biosynthesis. Nat. Commun. 9 (1), 2826. https://doi.org/10.1038/s41467-018-05221-5.
Komai, S., Hosoe, T., Itabashi, T., Nozawa, K., Okada, K., Campos Takaki, G.M., Yaguchi, T., Takizawa, K., Fukushima, K., Kawai, K., 2005. Two new meroterpenoids, penisimplicin A and B, isolated from *Penicillium simplicissimum*. Chem. Pharmaceut. Bull. 53 (9), 1114–1117. https://doi.org/10.1248/cpb.53.1114.
Kosalková, K., Domínguez-Santos, R., Coton, M., Coton, E., García-Estrada, C., Liras, P., Martín, J.F., 2015. A natural short pathway synthesizes roquefortine C but not meleagrin in three different *Penicillium roqueforti* strains. Appl. Microbiol. Biotechnol. 99 (18), 7601–7612. https://doi.org/10.1007/s00253-015-6676-0.
Kosemura, S., 2003. Meroterpenoids from *Penicillium citreo-viride* B. IFO 4692 and 6200 hybrid. Tetrahedron 59 (17), 5055–5072. https://doi.org/10.1016/S0040-4020(03)00739-7.
Kozlovsky, A.G., Kochkina, G.A., Zhelifonova, V.P., Antipova, T.V., Ivanushkina, N.E., Ozerskaya, S.M., 2020. Secondary metabolites of the genus *Penicillium* from undisturbed and anthropogenically altered Antarctic habitats. Folia Microbiol. 65 (1), 95–102. https://doi.org/10.1007/s12223-019-00708-0.
Landan, G., Graur, D., 2007. Heads or tails: a simple reliability check for multiple sequence alignments. Mol. Biol. Evol. 24 (6), 1380–1383. https://doi.org/10.1093/molbev/msm060.
Lassmann, T., Sonnhammer, E.L., 2005. Kalign-an accurate and fast multiple sequence alignment algorithm. BMC Bioinf. 6, 298. https://doi.org/10.1186/1471-2105-6-298.
Li, B., Zong, Y., Du, Z., Chen, Y., Zhang, Z., Qin, G., Zhao, W., Tian, S., 2015. Genomic characterization reveals insights into patulin biosynthesis and pathogenicity in *Penicillium* species. Molecular plant-microbe interactions: MPMI (Mol. Plant-Microbe Interact.) 28 (6), 635–647. https://doi.org/10.1094/MPMI-12-14-0398-FI.
Li, H.L., Xu, R., Li, X.M., Yang, S.Q., Meng, L.H., Wang, B.G., 2018. Simpterpenoid A, a meroterpenoid with a highly functionalized cyclohexadiene moiety featuring gem-Propane-1,2-dione and methylformate groups, from the mangrove-derived *Penicillium simplicissimum* MA-332. Org. Lett. 20 (5), 1465–1468. https://doi.org/10.1021/acs.orglett.8b00327.
Li, B., Chen, Y., Zong, Y., Shang, Y., Zhang, Z., Xu, X., Wang, X., Long, M., Tian, S., 2019. Dissection of patulin biosynthesis, spatial control and regulation mechanism in *Penicillium expansum*. Environ. Microbiol. 21 (3), 1124–1139. https://doi.org/10.1111/1462-2920.14542.
Lin, T.S., Chiang, Y.M., Wang, C.C., 2016. Biosynthetic pathway of the reduced polyketide product citreoviridin in *Aspergillus terreus* var. *aureus* revealed by heterologous expression in *Aspergillus nidulans*. Org. Lett. 18 (6), 1366–1369. https://doi.org/10.1021/acs.orglett.6b00299.
Liu, C., Tagami, K., Minami, A., Matsumoto, T., Frisvad, J.C., Suzuki, H., Ishikawa, J., Gomi, K., Oikawa, H., 2015. Reconstitution of biosynthetic machinery for the synthesis of the highly elaborated indole diterpene penitrem. Angew. Chem. 54 (19), 5748–5752. https://doi.org/10.1002/anie.201501072.
López, S.N., Sangorrín, M.P., Pildain, M.B., 2016. Fruit rot of sweet cherries and raspberries caused by *Penicillium crustosum* and *Mucor piriformis* in South Patagonia, Argentina. J. Indian Dent. Assoc. 38 (4), 511–516. https://doi.org/10.1080/07060661.2016.1243582.
Louw, J.P., Korsten, L., 2014. Pathogenic *Penicillium* spp. on apple and pear. Plant Dis. 98 (5), 590–598. https://doi.org/10.1094/PDIS-07-13-0710-RE.
Macheleidt, J., Mattern, D.J., Fischer, J., Netzker, T., Weber, J., Schroeckh, V., Valiante, V., Brakhage, A.A., 2016. Regulation and role of fungal secondary metabolites. Annu. Rev. Genet. 50, 371–392. https://doi.org/10.1146/annurev-genet-120215-035203.
Mansouri, S., Houbraken, J., Samson, R.A., Frisvad, J.C., Christensen, M., Tuthill, D.E., Koutaniemi, S., Hatakka, A., Lankinen, P., 2013. *Penicillium subrubescens*, a new species efficiently producing inulinase. Antonie Leeuwenhoek 103, 1343–1357. https://doi.org/10.1007/s10482-013-9915-3.
Matsuda, Y., Awakawa, T., Abe, I., 2013. Reconstituted biosynthesis of fungal meroterpenoid andrastin A. Tetrahedron 69 (38), 8199–8204. https://doi.org/10.1016/j.tet.2013.07.029.
Matsuda, Y., Iwabuchi, T., Fujimoto, T., Awakawa, T., Nakashima, Y., Mori, T., Zhang, H., Hayashi, F., Abe, I., 2016. Discovery of key dioxygenases that diverged the paraherquonin and acetoxydehydroaustin pathways in *Penicillium brasilianum*. J. Am. Chem. Soc. 138 (38), 12671–12677. https://doi.org/10.1021/jacs.6b08424.
Medema, M.H., Blin, K., Cimermancic, P., de Jager, V., Zakrzewski, P., Fischbach, M.A., Weber, T., Takano, E., Breitling, R., 2011. antiSMASH: rapid identification, annotation and analysis of secondary metabolite biosynthesis gene clusters in bacterial and fungal genome sequences. Nucleic Acids Res. 39 (Web Server issue), W339–W346. https://doi.org/10.1093/nar/gkr466.
Misihairabgwi, J.M., Ishola, A., Quaye, I., Sulyok, M., Krska, R., 2018. Diversity and fate of fungal metabolites during the preparation of oshikundu, a Namibian traditional fermented beverage. World Mycotoxin J. 11 (3), 471–481. https://doi.org/10.3920/WMJ2018.2352.
Nguyen, L.T., Schmidt, H.A., von Haeseler, A., Minh, B.Q., 2015. IQ-TREE: a fast and effective stochastic algorithm for estimating maximum-likelihood phylogenies. Mol. Biol. Evol. 32 (1), 268–274. https://doi.org/10.1093/molbev/msu300.
Nicholson, M.J., Eaton, C.J., Stärkel, C., Tapper, B.A., Cox, M.P., Scott, B., 2015. Molecular cloning and functional analysis of gene clusters for the biosynthesis of indole-diterpenes in *Penicillium crustosum* and *P. janthinellum*. Toxins 7 (8), 2701–2722. https://doi.org/10.3390/toxins7082701.
Nielsen, J.C., Grijseels, S., Prigent, S., Ji, B., Dainat, J., Nielsen, K.F., Frisvad, J.C., Workman, M., Nielsen, J., 2017. Global analysis of biosynthetic gene clusters reveals vast potential of secondary metabolite production in *Penicillium* species. Nature microbiology 2, 17044. https://doi.org/10.1038/nmicrobiol.2017.44.
Nielsen, M.T., Nielsen, J.B., Anyaogu, D.C., Holm, D.K., Nielsen, K.F., Larsen, T.O., Mortensen, U.H., 2013. Heterologous reconstitution of the intact geodin gene cluster

in *Aspergillus nidulans* through a simple and versatile PCR based approach. PLoS One 8 (8), e72871. https://doi.org/10.1371/journal.pone.0072871.
Okano, T., Kobayashi, N., Izawa, K., Yoshinari, T., Sugita-Konishi, Y., 2020. Whole genome analysis revealed the genes responsible for citreoviridin biosynthesis in *Penicillium citreonigrum*. Toxins 12 (2), 125. https://doi.org/10.3390/toxins12020125.
Olsen, M., Gidlund, A., Sulyok, M., 2017. Experimental mould growth and mycotoxin diffusion in different food items. World Mycotoxin J. 10, 153–161. https://doi.org/10.3920/WMJ2016.2163.
Olsen, M., Lindqvist, R., Bakeeva, A., Leong, S.L., Sulyok, M., 2019. Distribution of mycotoxins produced by *Penicillium* spp. inoculated in apple jam and crème fraiche during chilled storage. Int. J. Food Microbiol. 292, 13–20. https://doi.org/10.1016/j.ijfoodmicro.2018.12.003.
Overy, D.P., Seifert, K.A., Savard, M.E., Frisvad, J.C., 2003. Spoilage fungi and their mycotoxins in commercially marketed chestnuts. Int. J. Food Microbiol. 88 (1), 69–77. https://doi.org/10.1016/s0168-1605(03)00086-2.
Park, J.S., Quang, T.H., Yoon, C.S., Kim, H.J., Sohn, J.H., Oh, H., 2018. Furanoaustinol and 7-acetoxydehydroaustinol: new meroterpenoids from a marine-derived fungal strain *Penicillium* sp. SF-5497. J. Antibiot. 71 (6), 557–563. https://doi.org/10.1038/s41429-018-0034-2.
Paulino, D., Warren, R.L., Vandervalk, B.P., Raymond, A., Jackman, S.D., Birol, I., 2015. Sealer: a scalable gap-closing application for finishing draft genomes. BMC Bioinf. 16 (1), 230. https://doi.org/10.1186/s12859-015-0663-4.
Petersen, L.M., Holm, D.K., Gotfredsen, C.H., Mortensen, U.H., Larsen, T.O., 2015. Investigation of a 6-MSA synthase gene cluster in *Aspergillus aculeatus* reveals 6-MSA-derived aculinic acid, aculins A-B and epi-aculin A. Chembiochem: a European journal of chemical biology 16 (15), 2200–2204. https://doi.org/10.1002/cbic.201500210.
Prencipe, S., Siciliano, I., Gatti, C., Garibaldi, A., Gullino, M.L., Botta, R., Spadaro, D., 2018. Several species of *Penicillium* isolated from chestnut flour processing are pathogenic on fresh chestnuts and produce mycotoxins. Food Microbiol. 76, 396–404. https://doi.org/10.1016/j.fm.2018.07.003.
Qi, B.W., Li, N., Zhang, B.B., Zhang, Z.K., Wang, W.J., Liu, X., Wang, J., Awakawa, T., Tu, P.F., Abe, I., Shi, S.P., Li, J., 2022. A multifunctional cytochrome P450 and a meroterpenoid cyclase in the biosynthesis of fungal meroterpenoid atlantinone B. Org. Lett. 24 (13), 2526–2530. https://doi.org/10.1021/acs.orglett.2c00684.
Regueira, T.B., Kildegaard, K.R., Hansen, B.G., Mortensen, U.H., Hertweck, C., Nielsen, J., 2011. Molecular basis for mycophenolic acid biosynthesis in *Penicillium brevicompactum*. Appl. Environ. Microbiol. 77 (9), 3035–3043. https://doi.org/10.1128/AEM.03015-10.
Ren, Y., Chao, L.H., Sun, J., Chen, X.N., Yao, H.N., Zhu, Z.X., Dong, D., Liu, T., Tu, P.F., Li, J., 2019. Two new polyketides from the fungus *Penicillium oxalicum* MHZ153. Nat. Prod. Res. 33 (3), 347–353. https://doi.org/10.1080/14786419.2018.1452001.
Rodrigues, P., Venâncio, A., Lima, N., 2012. Mycobiota and mycotoxins of almonds and chestnuts with special reference to aflatoxins. Food Res. Int. 48 (1), 76–90. https://doi.org/10.1016/j.foodres.2012.02.007.
Rojas-Aedo, J.F., Gil-Durán, C., Del-Cid, A., Valdés, N., Álamos, P., Vaca, I., García-Rico, R.O., Levicán, G., Tello, M., Chávez, R., 2017. The biosynthetic gene cluster for andrastin A in *Penicillium roqueforti*. Front. Microbiol. 8, 813. https://doi.org/10.3389/fmicb.2017.00813.
Saikia, S., Parker, E.J., Koulman, A., Scott, B., 2006. Four gene products are required for the fungal synthesis of the indole-diterpene, paspaline. FEBS Lett. 580 (6), 1625–1630. https://doi.org/10.1016/j.febslet.2006.02.008.
Schoch, C.L., Ciufo, S., Domrachev, M., Hotton, C.L., Kannan, S., Khovanskaya, R., Leipe, D., Mcveigh, R., O'Neill, K., Robbertse, B., Sharma, S., Soussov, V., Sullivan, J. P., Sun, L., Turner, S., Karsch-Mizrachi, I., 2020. NCBI Taxonomy: a comprehensive update on curation, resources and tools. Database: the journal of biological databases and curation 2020, baaa062. https://doi.org/10.1093/database/baaa062.
Smetanina, O.F., Kalinovsky, A.I., Khudyakova, Y.V., Pivkin, M.V., Dmitrenok, P.S., Fedorov, S.N., Ji, H., Kwak, J.Y., Kuznetsova, T.A., 2007. Indole alkaloids produced by a marine fungus isolate of *Penicillium janthinellum* Biourge. J. Nat. Prod. 70 (6), 906–909. https://doi.org/10.1021/np060396d.
Snini, S.P., Tadrist, S., Laffitte, J., Jamin, E.L., Oswald, I.P., Puel, O., 2014. The gene PatG involved in the biosynthesis pathway of patulin, a food-borne mycotoxin, encodes a 6-methylsalicylic acid decarboxylase. Int. J. Food Microbiol. 171, 77–83. https://doi.org/10.1016/j.ijfoodmicro.2013.11.020.
Sonjak, S., Frisvad, J.C., Gunde-Cimerman, N., 2005. Comparison of secondary metabolite production by *Penicillium crustosum* strains, isolated from Arctic and other various ecological niches. FEMS (Fed. Eur. Microbiol. Soc.) Microbiol. Ecol. 53, 51–60. https://doi.org/10.1016/j.femsec.2004.10.014.
Spadaro, D., Meloni, G.R., Siciliano, I., Prencipe, S., Gullino, M.L., 2020. HPLC-MS/MS method for the detection of selected toxic metabolites produced by *Penicillium* spp. in nuts. Toxins 12 (5), 307. https://doi.org/10.3390/toxins12050307.
Stanke, M., Keller, O., Gunduz, I., Hayes, A., Waack, S., Morgenstern, B., 2006. AUGUSTUS: ab initio prediction of alternative transcripts. Nucleic Acids Res. 34 (Web Server issue), W435–W439. https://doi.org/10.1093/nar/gkl200.
Stierle, D.B., Stierle, A.A., Patacini, B., McIntyre, K., Girtsman, T., Bolstad, E., 2011. Berkeleyones and related meroterpenes from a deep water acid mine waste fungus that inhibit the production of interleukin 1-β from induced inflammasomes. J. Nat. Prod. 74 (10), 2273–2277. https://doi.org/10.1021/np2003066.
Sumarah, M.W., Miller, J.D., Blackwell, B.A., 2005. Isolation and metabolite production by *Penicillium roqueforti, P. paneum* and *P. crustosum* isolated in Canada. Mycopathologia 159 (4), 571–577. https://doi.org/10.1007/s11046-005-5257-7.
Sun, J., Zhu, Z.X., Song, Y.L., Dong, D., Zheng, J., Liu, T., Zhao, Y.F., Ferreira, D., Zjawiony, J.K., Tu, P.F., Li, J., 2016. Nitric oxide inhibitory meroterpenoids from the fungus *Penicillium purpurogenum* MHZ 111. J. Nat. Prod. 79 (5), 1415–1422. https://doi.org/10.1021/acs.jnatprod.6b00160.
Taevernier, L., Wynendaele, E., De Vreese, L., Burvenich, C., De Spiegeleer, B., 2016. The mycotoxin definition reconsidered towards fungal cyclic depsipeptides. Journal of Environmental Science and Health, Part C 34 (2), 114–135. https://doi.org/10.1080/10590501.2016.1164561.
Tang, M.C., Cui, X., He, X., Ding, Z., Zhu, T., Tang, Y., Li, D., 2017. Late-stage terpene cyclization by an integral membrane cyclase in the biosynthesis of isoprenoid epoxycyclohexenone natural products. Org. Lett. 19 (19), 5376–5379. https://doi.org/10.1021/acs.orglett.7b02653.
Tannous, J., El Khoury, R., Snini, S.P., Lippi, Y., El Khoury, A., Atoui, A., Lteif, R., Oswald, I.P., Puel, O., 2014. Sequencing, physical organization and kinetic expression of the patulin biosynthetic gene cluster from *Penicillium expansum*. Int. J. Food Microbiol. 189, 51–60. https://doi.org/10.1016/j.ijfoodmicro.2014.07.028.
Tannous, J., Snini, S.P., El Khoury, R., Canlet, C., Pinton, P., Lippi, Y., Alassane-Kpembi, I., Gauthier, T., El Khoury, A., Atoui, A., Zhou, T., Lteif, R., Oswald, I.P., Puel, O., 2017. Patulin transformation products and last intermediates in its biosynthetic pathway, E- and Z-ascladiol, are not toxic to human cells. Arch. Toxicol. 91 (6), 2455–2467. https://doi.org/10.1007/s00204-016-1900-y.
Thomas, S., Sharma, N., Gonzalez, R., Pao, P.W., Hofman, F.M., Chen, T.C., Louie, S.G., Pirrung, M.C., Schönthal, A.H., 2013. Repositioning of Verrucosidin, a purported inhibitor of chaperone protein GRP78, as an inhibitor of mitochondrial electron transport chain complex I. PLoS One 8 (6), e65695. https://doi.org/10.1371/journal.pone.0065695.
Throckmorton, K., Lim, F.Y., Kontoyiannis, D.P., Zheng, W., Keller, N.P., 2016. Redundant synthesis of a conidial polyketide by two distinct secondary metabolite clusters in Aspergillus fumigatus. Environ. Microbiol. 18 (1), 246–259. https://doi.org/10.1111/1462-2920.13007.
UniProt Consortium, 2019. UniProt: a worldwide hub of protein knowledge. Nucleic Acids Res. 47 (D1), D506–D515. https://doi.org/10.1093/nar/gky1049.
Valente, S., Piombo, E., Schroeckh, V., Meloni, G.R., Heinekamp, T., Brakhage, A.A., Spadaro, D., 2021. CRISPR-Cas9-Based discovery of the verrucosidin biosynthesis gene cluster in *Penicillium polonicum*. Front. Microbiol. 12, 660871 https://doi.org/10.3389/fmicb.2021.660871.
van den Berg, M.A., Albang, R., Albermann, K., Badger, J.H., Daran, J.M., Driessen, A.J., Garcia-Estrada, C., Fedorova, N.D., Harris, D.M., Heijne, W.H., Joardar, V., Kiel, J.A., Kovalchuk, A., Martín, J.F., Nierman, W.C., Nijland, J.G., Pronk, J.T., Roubos, J.A., van der Klei, I.J., van Peij, N.N., et al., 2008. Genome sequencing and analysis of the filamentous fungus *Penicillium chrysogenum*. Nat. Biotechnol. 26 (10), 1161–1168. https://doi.org/10.1038/nbt.1498.
Vansteelandt, M., Kerzaon, I., Blanchet, E., Fossi Tankoua, O., Robiou Du Pont, T., Joubert, Y., Monteau, F., Le Bizec, B., Frisvad, J.C., Pouchus, Y.F., Grovel, O., 2012. Patulin and secondary metabolite production by marine-derived *Penicillium* strains. Fungal Biol. 116 (9), 954–961. https://doi.org/10.1016/j.funbio.2012.06.005.
Visagie, C.M., Frisvad, J.C., Houbraken, J., Visagie, A., Samson, R.A., Jacobs, K., 2021. A re-evaluation of *Penicillium* section Canescentia, including the description of five new species. Persoonia 46, 163–187. https://doi.org/10.3767/persoonia.2021.46.06.
Visagie, C.M., Houbraken, J., Frisvad, J.C., Hong, S.B., Klaassen, C.H., Perrone, G., Seifert, K.A., Varga, J., Yaguchi, T., Samson, R.A., 2014. Identification and nomenclature of the genus *Penicillium*. Stud. Mycol. 78, 343–371. https://doi.org/10.1016/j.simyco.2014.09.001.
Wallace, I.M., O'Sullivan, O., Higgins, D.G., Notredame, C., 2006. M-Coffee: combining multiple sequence alignment methods with T-Coffee. Nucleic Acids Res. 34 (6), 1692–1699. https://doi.org/10.1093/nar/gkl091.
Wang, J.F., Zhou, L.M., Chen, S.T., Yang, B., Liao, S.R., Kong, F.D., Lin, X.P., Wang, F.Z., Zhou, X.F., Liu, Y.H., 2018. New chlorinated diphenyl ethers and xanthones from a deep-sea-derived fungus *Penicillium chrysogenum* SCSIO 41001. Fitoterapia 125, 49–54. https://doi.org/10.1016/j.fitote.2017.12.012.
Wehe, A., Bansal, M.S., Burleigh, J.G., Eulenstein, O., 2008. DupTree: a program for large-scale phylogenetic analyses using gene tree parsimony. Bioinformatics 24 (13), 1540–1541. https://doi.org/10.1093/bioinformatics/btn230.
Wigmann, É.F., Saccomori, F., Bernardi, A.O., Frisvad, J.C., Copetti, M.V., 2015. Toxigenic penicillia spoiling frozen chicken nuggets. Food Res. Int. 67, 219–222. https://doi.org/10.1016/j.foodres.2014.11.025.
Xu, M., Gessner, G., Groth, I., Lange, C., Christner, A., Bruhn, T., Deng, Z., Li, X., Heinemann, S.H., Bringmann, G., Grabley, S., Sattler, I., Lin, W., 2007. Shearinines D–K, new indole triterpenoids from an endophytic *Penicillium* sp. (strain HKI0459) with blocking activity on large-conductance calcium-activated potassium channels. Tetrahedron 63 (2), 435–444. https://doi.org/10.1016/j.tet.2006.10.050.
Yin, G., Zhang, Y., Pennerman, K.K., Wu, G., Hua, S.S.T., Yu, J., Jurick, W.M., Guo, A., Bennett, J.W., 2017. Characterization of blue mold Penicillium species isolated from stored fruits using multiple highly conserved loci. Journal of fungi 3 (1), 12. https://doi.org/10.3390/jof3010012.
Zetina-Serrano, C., Rocher, O., Naylies, C., Lippi, Y., Oswald, I.P., Lorber, S., Puel, O., 2020. The *brlA* gene deletion reveals that patulin biosynthesis is not related to conidiation in *Penicillium expansum*. Int. J. Mol. Sci. 21 (18), 6660. https://doi.org/10.3390/ijms21186660.
Zhang, J., Yuan, B., Liu, D., Gao, S., Proksch, P., Lin, W., 2018. Brasilianoids A-F, new meroterpenoids from the sponge-associated fungus *Penicillium brasilianum*. Front. Chem. 6, 314. https://doi.org/10.3389/fchem.2018.00314.
Zhang, W., Cao, S., Qiu, L., Qi, F., Li, Z., Yang, Y., Huang, S., Bai, F., Liu, C., Wan, X., Li, S., 2015. Functional characterization of MpaG', the O-methyltransferase involved in the biosynthesis of mycophenolic acid. Chembiochem: a European journal of chemical biology 16 (4), 565–569. https://doi.org/10.1002/cbic.201402600.

Zhang, W., Du, L., Qu, Z., Zhang, X., Li, F., Li, Z., Qi, F., Wang, X., Jiang, Y., Men, P., Sun, J., Cao, S., Geng, C., Qi, F., Wan, X., Liu, C., Li, S., 2019. Compartmentalized biosynthesis of mycophenolic acid. Proc. Natl. Acad. Sci. U.S.A. 116 (27), 13305–13310. https://doi.org/10.1073/pnas.1821932116.

Zhong, L., Carere, J., Lu, Z., Lu, F., Zhou, T., 2018. Patulin in apples and apple-based food products: the burdens and the mitigation strategies. Toxins 10 (11), 475. https://doi.org/10.3390/toxins10110475.

Zou, Y., Zhan, Z., Li, D., Tang, M., Cacho, R.A., Watanabe, K., Tang, Y., 2015. Tandem prenyltransferases catalyze isoprenoid elongation and complexity generation in biosynthesis of quinolone alkaloids. J. Am. Chem. Soc. 137 (15), 4980–4983. https://doi.org/10.1021/jacs.5b03.